4-Component relativistic calculations of L3 ionization and excitations for the isoelectronic species UO22+, OUN+ and UN2

Christopher South, Avijit Shee, Debashis Mukherjee, Angela K. Wilson, Trond Saue

4-component relativistic calculations of L_3 ionization and excitations for the isoelectronic species UO_2^{2+}, OUN^+ and UN_2

Christopher South[1)], Avijit Shee[2)], Debashis Mukherjee[3)], Angela K. Wilson[1,4)] and Trond Saue[2)*]

January 28, 2020

1) Department of Chemistry and Center for Advanced Scientific Computation and Modeling (CASCaM), University of North Texas, 1155 Union Circle #305070, Denton, TX 76203-5017, United States
2) Laboratoire de Chimie et Physique Quantiques, UMR 5626 CNRS — Université Toulouse III-Paul Sabatier 118 route de Narbonne, F-31062 Toulouse, France
3) Raman Center for Atomic, Molecular and Optical Sciences, Indian Association for the Cultivation of Science, Kolkata 700 032, India
4) Department of Chemistry, Michigan State University, East Lansing, Michigan 48824-1322
*) Corresponding author: trond.saue@irsamc.ups-tlse.fr

Abstract

We present a 4-component relativistic study of uranium $2p_{3/2}$ ionization and excitation in the isoelectronic series UO_2^{2+}, OUN^+ and UN_2. We calculate ionization energies by ΔSCF at the Hartree-Fock(HF) and Kohn-Sham(KS) level of theory. At the ΔHF level we observe a perfectly linear chemical shift of ionization energies with respect to uranium atomic charges obtained from projection analysis. We have also developed a non-canonical 2nd-order Møller-Plesset code for wave function based correlation studies. We observe the well-known failure of Koopmans' theorem for core ionization due to the dominance of orbital relaxation over electron correlation effects. More unexpectedly, we find that the correlation contribution has the same sign as the relaxation contribution and show that this is due to a strong coupling of relaxation and correlation. We simulate uranium L_3 XANES spectra, dominated by $2p_{3/2} \rightarrow U6d$ transitions, by restricted excitation window time-dependent density functional theory (REW-TDDFT) and the complex polarization propagator (CPP) approach and demonstrate that they give identical spectra when the same Lorentz broadening is chosen. We also simulate XANES spectra by the Hartree-Fock based static exchange (STEX) method and show how STEX excitation energies can be reproduced by time-dependent Hartree-Fock calculations within the Tamm-Dancoff approximation. We furthermore show that Koopmans' theorem provide a correct approximation of ionization energies in the linear response regime and use this observation to align REW-TDDFT and CPP spectra with STEX ones. We point out that the STEX method affords the most detailed assignment of spectra since it employs virtual orbitals optimized for the selected core ionization. The calculated XANES spectra reflect the loss of bound virtual orbitals as the molecular charge is reduced along the isoelectronic series.

1 Introduction

Uranyl compounds are of great interest due to their unique coordination chemistry as well as their potential impact on the environment. Uranium has been shown to readily form a myriad of coordination complexes in three separate oxidation states (IV, V, and VI), though tends to prefer

the IV and VI oxidation states, resulting in its rich chemistry [1–4]. Because uranium (along with thorium, actinium, and protactinium) is one of the few actinide elements that is stable and safe enough to be characterized in a laboratory, this allows for the physical effects of the f orbitals on the electronic structure, geometry and thermochemistry to be determined experimentally, giving much insight on the electronic structure of uranyl coordination complexes. [5–15]

The electronic properties of uranyl coordination complexes, as well as the nature of the compounds themselves, have been determined through electronic spectroscopy and x-ray diffraction methods. X-ray absorbance and photoelectron spectroscopy have been frequently used to provide knowledge about the electronic structure of the deep core, which results in an element specific electronic spectrum[7]. X-ray absorbance near edge spectroscopy (XANES) has been used to probe low lying unoccupied core ionized states of the uranyl complexes, returning energetics of the energy levels of the low lying virtual orbitals, as well as information on the oxidation state of the molecule[7, 9, 14, 15]. Walshe and coworkers used both high resolution XANES spectroscopy as well as extended X-ray absorbance fine structure (EXAFS) spectroscopy to characterize uranyl peroxides and uranyl oxohydroxides in their mineral forms and provided the first experimental crystal structure of metastudtite, as well as subtle differences in the core spectra of the mineral forms studied[14]. Given the highly local nature of the atomic core orbitals, the orbitals will be heavily affected by changes in the local electronic environment, such as relaxation effects which may be caused by changes in the formal oxidation state.

While uranium is not strongly radioactive (an alpha emitter with a half-life of over 44 billion years), it still presents a significant long term health risk, especially in a solvated form such as uranyl[16]. Computational modeling of uranium complexes circumvents this risk and has been used to model the thermochemistry and electronic structure of uranium coordination complexes[12, 17–32].

Analogous to experiment, computational chemistry can be used to calculate electronic transitions, allowing for the creation of electronic spectra from calculated excitation energies. Multi-reference computational methods have been used to directly solve for electronic states and transitions between states in the molecule[23–25, 28]. Reál *et al.* compared preexisting CASPT2 electronic transitions of uranyl to intermediate Hamiltonian Fock space coupled cluster (IHF-SCC) excitations and found that the two methods perform similarly for low level excitations, but the methods deviate from each other for higher excitation energies[25]. However, multi-reference methods scale unfavorably with the size of the system, and as a result, can only be utilized for the smallest of molecular systems. A commonly used alternative to multi-reference methods for the simulation of molecular spectra is time-dependent DFT (TDDFT), which have been used to great effect to calculate the electronic transitions in uranyl complexes[23, 33–35]. Tecmer *et al.* performed TDDFT calculations to simulate the UV-Vis spectrum of uranyl as well as the isoelectronic analogues OUN^+ and UN_2. They found that among the functionals used, CAMB3LYP, M06, and PBE0 gave the lowest mean errors relative to IHFSCC, performing similarly to CASPT2 overall[34]. The complex polarization propagator (CPP) method[36–41] is similar to time-dependent methods, but explicitly accounts for the linewidth of the peaks via an imaginary damping factor which, when graphed, generates the spectrum. At the Hartree-Fock level, the static exchange approximation (STEX)[42–44] models core excitations as an electron being acted upon by the core ionized molecule, the latter of which is optimized separately in order to give a complete account of the orbital relaxation in the molecule.

Accounting for relativistic effects is of great importance in calculations on actinide elements, especially in the calculation of properties of deep core orbitals as spin-orbit is incredibly strong for these orbitals. The most direct means of accounting for relativity is the full four-component Dirac-Coulomb (DC) Hamiltonian. The DC Hamiltonian gives a full account of the one-electron relativistic effects in a molecule, whereas the fully relativistic two-electron interaction is truncated, but includes the instantaneous Coulomb interaction as well as spin-own orbit interaction.[45] It has been used to calculate properties of uranyl and its complexes [20, 24, 25]. Relativistic effective core potentials (RECPs) are another means of accounting for relativistic effects for heavy atoms, and have been used frequently to recover these effects and to simplify the costly calculations involved [12, 18, 23, 25, 26, 32, 35, 46–49]. Dolg and Cao developed a relativistic small core

pseudopotential for uranium constructed from Dirac-Coulomb-Breit (DCB) orbitals, compared it to all-electron DKH calculations with perturbative spin-orbit (+BP), and noted that the vertical excitation energies agreed well with the values obtained at the all-electron level, at far reduced computational cost [46]. However, since the chemical core is simplified and treated by a simple function, part of the core level description is lost and no core level properties (such as core-ionization energies) can be calculated. The large and small component of the wave function can also be decoupled yielding two (or one) component Hamiltonians for the purpose of reducing computational cost relative to the full four-component calculation [22, 23, 25, 28, 29, 33]. The eXact 2-Component relativistic Hamiltonian (X2C)[50–52] has been used by Reál et al. to calculate relativistic effects for uranyl compounds and has resulted in similar effectiveness to Dirac-Coulomb in the calculation of vertical excitation energies[25]. Klooster *et al.* [53] have reported calculations of X-ray photoelectron spectra, including U^{5+} using the analogous normalized elimination of the small component (NESC) Hamiltonian. Calculations on uranium compounds including scalar relativistic effects through the Darwin and mass−velocity terms have also been reported[29, 31].

Two isoelectronic homologues of uranyl have been synthesized, OUN^+ and UN_2, and have been characterized using experimental and theoretical methods[23, 31, 32, 34, 47, 54]. Both of these molecules possess uranium in the +6 formal oxidation state and, analogous to uranyl, have also been shown to have linear structures [17, 23, 26, 29, 31, 32, 34, 47, 48, 55, 56]. The geometries and valence electronic spectra for these molecules have been determined computationally. However, less is known about the core spectra of these molecules from a theoretical standpoint (especially for OUN^+ and UN_2).

Therefore, to classify and characterize these new molecules, we have in the present work simulated the uranium L_3 edge XANES spectrum for UO_2^{2+}, OUN^+ and UN_2 using restricted excitation window (REW) TDDFT, the CPP method, as well as STEX. We have also investigated the position of the uranium L_3 ionization threshold using both wave function and density functional methods. The paper is outlined as follows: In section 2 we present the theory behind the methods employed in this work. In section 3 we provide computational details and then, in section 4, present and discuss our results. In section 5 we provide conclusions and perspectives.

2 Theory

2.1 Core ionization

Koopmans' theorem [57] provides a reasonable estimate of valence ionization energies, although it is based on the difference of Hartree-Fock energies between the ionized and the parent state, using the orbitals of the parent state. There are accordingly two major sources of error, that is, i) lack of orbital relaxation of the core-ionized state and ii) lack of electron correlation:

$$IP_i\left(M\right) = -\varepsilon_i\left(M\right) + \Delta_{relax} + \Delta_{corr}.$$

The relaxation contribution Δ_{relax} ($-\Delta_{relax}$ is denoted the contraction error by Koopmans [57]) will be negative since orbital relaxation lowers the energy of the core-ionized state. The correlation contribution Δ_{corr} is, on the other hand, expected to be positive since there is one more electron to correlate in the parent state (see for instance [58]). In practice, for valence ionizations, the two contributions are found to be of the same order of magnitude, there by providing fortunate error cancellation, as illustrated for the HOMO ($1b_1$) ionization of the water molecule in table 1. For core ionizations, on the other hand, the Koopmans estimate is known to be poor[59] since the correlation contribution is typically an order of magnitude smaller than the relaxation contribution, as seen in table 1 for the $1a_1$ (oxygen 1s) ionization energy.

In the present work the correlation contribution is calculated by ΔMP2. The core-ionized state is first obtained by a Kramers restricted average-of-configuration Hartree-Fock (HF) calculation[62] starting from the orbitals of the parent state. Convergence is straightforward and obtained by first

Method	$1b_1^{-1}$	$1a_1^{-1}$
Exp.	12.61[60]	539.7[61]
Koopmans	13.84	560.1
ΔHF	11.05	539.6
ΔMP2	12.75	540.5
Δ_{relax}	-2.79	-20.5
Δ_{corr}	1.70	0.9

Table 1: *Valence and core ionization energies (in eV) of gaseous water obtained using the dyall.ae3z basis set.*

reordering the orbitals such that the target core orbital is in the position of the open shell and then kept there by overlap selection. This method has been used since the molecular ΔSCF calculations of Bagus and Schaefer [63, 64], but has more recently been rediscovered under the name Maximum Overlap Method by Gill and co-workers[65]. For the ΔMP2 calculation we have employed the RELCCSD module of DIRAC [66] which uses an Kramers unrestricted formalism[67] and thereby allows simple open-shell calculations. However, since the incoming molecular orbitals are optimized under Kramers restriction, the reconstructed Fock matrix for the core-ionized state is not diagonal and will have have a non-zero occupied-virtual (ov) block. We have therefore extended the MP2 algorithm to handle this case. We start from the electronic Hamiltonian normal-ordered with respect to the Fermi vacuum defined by the current (Kramers restricted) orbital set

$$H_N = \sum_{pq} f_q^p \left\{a_p^\dagger a_q\right\} + \frac{1}{4}\sum_{pqrs} V_{qs}^{pr} \left\{a_p^\dagger a_r^\dagger a_s a_q\right\}; \quad V_{qs}^{pr} = \langle pr \,||\, qs\rangle \,.$$

Following Lauderdale *et al.* [68], we then define the zeroth-order Hamiltonian to be the diagonal blocks (oo and vv) of the Fock matrix. Setting up perturbation theory in a coupled cluster (CC) framework we subsequently derive the non-canonical MP2 energy

$$E^{ncMP2} = \sum_{ai} f_a^i t_i^{a(1)} + \frac{1}{4}\sum_{ij}\sum_{ab} V_{ab}^{ij} t_{ij}^{ab(1)}. \tag{1}$$

Here and in the following we employ indices i, j, k, l for occupied orbitals, a, b, c, d for virtual orbitals and p, q, r, s for general orbitals. The equations of the first-order CC amplitudes are

$$\begin{aligned} \sum_b f_b^a t_i^{b(1)} - \sum_j t_j^{a(1)} f_i^j &= -f_i^a \\ \sum_c \left(f_c^b t_{ij}^{ac(1)} + f_c^a t_{ij}^{bc(1)}\right) - \sum_k \left(f_j^k t_{ik}^{ab(1)} + f_i^k t_{jk}^{ab(1)}\right) &= -V_{ij}^{ab}. \end{aligned}$$

Starting from these, one may show that the non-canonical MP2 energy is invariant under separate rotation of occupied and virtual orbitals. The equation for the first-order T_1-amplitudes may be recognized as the Sylvester equation and can therefore be solved in a direct fashion, but we have for convenience chosen to use the existing iterative scheme in RELCCSD for the solution of the amplitude equations.

2.2 Core excitation

In this work we are exploring three different methods for the calculation of core excitation spectra: restricted excitation window time-dependent density functional theory (REW-TDDFT), complex polarization propagator (CPP) and the static exchange approximation (STEX). In this section we give a brief presentation and comparison of these methods.

A common starting point for the three methods is the frequency-dependent linear response function which in the exact state formalism[69–71]

$$\langle\langle A;B\rangle\rangle_\omega = -\frac{1}{\hbar}\sum_{m>0}\left\{\frac{A_m^* B_m}{\omega_m-\omega}+\frac{B_m^* A_m}{\omega_m+\omega}\right\} \tag{2}$$

involves an explicit sum over the excited states $|m\rangle$ of the zeroth-order Hamiltonian. In the above expression $\hbar\omega_m = E_m - E_0$ are excitation energies with respect to the unperturbed ground state $|0\rangle$ and $P_m = \left\langle m\left|\hat{H}_P\right|0\right\rangle$, $(P=A,B)$ the corresponding transition moments with respect to property operator $\hat{H}_P$. In the present work we restrict ourselves to the electric dipole approximation, so that both property operators are limited to components of the electric dipole operator, although the short wave length of X-ray radiation may require the inclusion of terms beyond this approximation [72, 73]. It is clear from the above expression that a scan of the linear response function through a frequency window will display poles corresponding to excitations in the range allowed by the property operators $\hat{H}_A$ and $\hat{H}_B$ and whose transition moments can be extracted from the residues. The singularities are unphysical, though, in that they correspond to infinitely long lifetimes of the excited states. This feature may be amended by the introduction of inverse lifetimes γ_m through the substitution $\omega_m \to \omega_m - i\gamma_m$ in the above expression (2). The response function then becomes generally complex, with the real part corresponding to refractive properties such as polarizabilities and the imaginary part associated with absorption processes.

Within the framework of Hartree-Fock and Kohn-Sham methods we may employ an exponential parametrization of orbitals (and thereby density and energy)

$$\varphi_i(\boldsymbol{\kappa}) = \sum_a \varphi_a \exp\left[-\kappa\right]_{ai}; \quad \kappa_{pq} = -\kappa_{qp}^*$$

which allows for unconstrained optimization and straightforward identification of redundancies [74–77]. In the present case we restrict ourselves to closed-shell references in which only rotations between occupied and virtual orbitals, with amplitudes κ_{ai}, are non-redundant; all other amplitudes may therefore be set to zero. At the SCF level of theory the frequency-dependent linear response function may be formulated as

$$\langle\langle A;B\rangle\rangle_\omega = \boldsymbol{E}_A^{[1]\dagger}\boldsymbol{X}_B(\omega),$$

where the vector $\boldsymbol{X}_B(\omega)$ contains the first-order orbital rotation amplitudes

$$\mathbf{X}_B(\omega) = \begin{bmatrix} \mathbf{K}(\omega) \\ \mathbf{K}^*(-\omega) \end{bmatrix}; \quad K_{ai}(\omega) = \kappa_{ai}^{(1)}(\omega).$$

It is a solution of the linear response equation

$$\left(E_0^{[2]} - \hbar\omega S^{[2]}\right)\mathbf{X}_B(\omega) = -\mathbf{E}_B^{[1]},$$

where appears the property gradient

$$\mathbf{E}_B^{[1]} = \begin{bmatrix} \boldsymbol{g} \\ \boldsymbol{g}^* \end{bmatrix}; \quad g_{ai} = -\left\langle\varphi_a\left|\hat{H}_B\right|\varphi_i\right\rangle$$

as well as the the generalized metric $S^{[2]}$ and the electronic Hessian $E_0^{[2]}$, with structures

$$S^{[2]} = \begin{bmatrix} I & 0 \\ 0 & -I \end{bmatrix}; \quad E_0^{[2]} = \begin{bmatrix} A & B \\ B^* & A^* \end{bmatrix}; \qquad \begin{aligned} A_{ai,bj} &= \left.\frac{\partial^2 E_0}{\partial\kappa_{ai}^*\partial\kappa_{bj}}\right|_{\boldsymbol{\kappa}=\mathbf{0}} \\ B_{ai,bj} &= \left.\frac{\partial^2 E_0}{\partial\kappa_{ai}^*\partial\kappa_{bj}^*}\right|_{\boldsymbol{\kappa}=\mathbf{0}} \end{aligned}. \tag{3}$$

Further discussion of the SCF linear response formalism can be for instance be found in references [69, 78, 79]. Since the SCF linear response function do not contain any sum over states, its complex extension can not be obtained by the introduction of state-specific inverse lifetimes γ_m. It is therefore common practice to employ a single damping parameter γ which can be interpreted as an imaginary extension of the perturbing frequency $\omega \rightarrow \omega + i\gamma$ [36–41]. A relativistic implementation of complex response, including spin-orbit interaction, has been reported by Devarajan et al. [39]. However, it is based on the zeroth order regular approximation (ZORA), which may not be very accurate for core excitations, as pointed out by the authors themselves. In the present contribution we employ the complex response implementation of the DIRAC code[80], which can be used with the more accurate 4-component Dirac-Coulomb and eXact 2-Component (X2C) Hamiltonians. Working within the electric dipole approximation the isotropic oscillator strength f^{iso}, including a Lorentzian linewidth defined by the damping parameter γ, is obtained directly by a scan of the imaginary part of the isotropic electric dipole polarizability α^{iso} through the desired frequency window

$$f^{iso}(\omega) = \frac{2m\omega}{\pi e^2} Im\left\{\alpha^{iso}(\omega + i\gamma)\right\}.$$

Alternatively, excitation energies can be found by TDDFT (or TDHF), that is, by solving the generalized eigenvalue problem

$$\left(E_0^{[2]} - \hbar\omega_m S^{[2]}\right)\mathbf{X}_m = 0.$$

An inconvenience with this approach is that excitation energies are typically found by a "bottom-up" approach, which becomes highly impractical for core excitations. A solution is to restrict the occupied orbitals entering the orbitals rotation amplitudes $\{\kappa_{ai}\}$ to the desired core orbitals. This is referred to a the "restricted excitation window"[81] or "restricted channel"[82] approach. In the present work we employ the relativistic adiabatic TDDFT implementation reported by Bast *et al.*[71], where restriction are possible both on occupied and virtual orbitals, such that the extension to REW-TDDFT is straightforward.

Transition moments are found by contracting the eigenvectors $\mathbf{X}_m$ with the corresponding property gradient

$$P_m = \mathbf{X}_m^{\dagger}(\omega)\boldsymbol{E}_P^{[1]}.$$

The isotropic oscillator strength associated with excitation m is then obtained as

$$f_m^{iso} = \frac{2m\omega_m}{3\hbar e^2}\sum_{\alpha=x,y,z}\left|\mu_{m,\alpha}\right|^2. \tag{4}$$

Cumulated isotropic oscillator strengths, including a Lorentzian broadening Δ^L, are then obtained as

$$f^{iso}(\omega) = \sum_m f_m^{iso}\Delta^L(\omega;\omega_m,\gamma); \quad \Delta^L(\omega;\omega_m,\gamma) = \frac{1}{\gamma\pi}\left[\frac{\gamma^2}{(\omega-\omega_m)^2+\gamma^2}\right].$$

The resulting simulated spectra obtained by complex response and REW-TDDFT are expected to be identical to the extent that no other occupied orbitals are involved in the excitation processes with the selected frequency window (channel coupling) and to the extent that the REW-TDDFT calculation includes a sufficient number of excitation to cover the frequency window. In passing we note that upon a change of energy units the Lorentz-broadened oscillators strengths are scaled down by the same factor as the energy is scaled up, in order to conserve the integrated oscillator strength.

A third method investigated in the present work is the static exchange approximation (STEX). The name originated in the context of early theoretical investigations of the scattering of electrons by hydrogen atoms[83, 84]. The two-electron wave function of the system was expanded in products of hydrogen atom orbitals and orbitals of the projectile electron[85]. The static exchange approximation was obtained by restricting the atomic orbital in this expansion to the ground state $1s$ orbital of the target hydrogen atom, thus neglecting polarization of the atomic charge

density during collision, yet retaining exchange effects, shown by Morse and Allis in 1933 to have some importance upon scattering with slow electrons [86]. This is apparently the first STEX calculation. A further development was the observation by Hunt and Goddard[87] that the optimal virtual orbital φ_a in the otherwise frozen N-electron singly-excited determinant Φ_i^a is obtained by diagonalization of the orbital-specific Fock operator

$$\hat{F}^{(N-i)} = \hat{h} + \sum_{j\neq i}^{N} \left(\hat{J}_j - \hat{K}_j \right)$$

where $\hat{J}_j$ and $\hat{K}_j$ are the usual Coulomb and exchange operators, respectively. The diagonalization is carried out in the space of virtual orbitals, thus keeping the occupied orbitals frozen. The assumption that the other occupied orbitals are hardly modified upon excitation is an instance of the STEX approximation, as pointed out by Langhoff[88–90]. The so-called improved virtual orbitals (IVO) generated in this manner contrasts with the canonical virtual HF orbitals generated from the usual Fock operator

$$\hat{F}^{N} = \hat{F}^{(N-i)} + \left(\hat{J}_i - \hat{K}_i \right)$$

and which are more appropriate for the $(N+1)$-electron system. Not surprisingly then, the orbital-specific Fock operator $\hat{F}^{(N-i)}$ is also the conventional Fock operator for the $(N-1)$-electron system obtained by removal of the occupied orbital φ_i from the system. Based on the above observations, Ågren and co-workers [42, 43] proposed to extend the IVO approach to core excitations and notably to build the STEX operator $\hat{F}^{(N-i)}$ using the occupied orbitals of the corresponding core ionized system, thus capturing orbital relaxation essentially missing in TD-DFT/HF. Transition moments are calculated between the parent ground state and the core excited states, the latter built from the core ionized orbitals. Since two non-orthogonal orbital sets are used, special techniques, such as a cofactor expansion [91], must be used. In the present work we are using the 4-component relativistic STEX implementation of Ekström *et al.* [92].

The core excitation energies obtained by a STEX calculation can be reproduced by a REW-TDHF calculation using the orbitals of the core ionized system and invoking the Tamm-Dancoff approximation (TDA), that is, setting $B = 0$ in the electronic Hessian (3). If excitations are restricted to a single (core) orbital φ_i the elements of the remaining A block can be expressed as

$$\begin{aligned} A_{ai,bi} &= \left\langle \tilde{\Phi}_i^a \middle| \hat{H}^N \middle| \tilde{\Phi}_i^b \right\rangle - \delta_{ab} \left\langle \tilde{\Phi}_0 \middle| \hat{H}^N \middle| \tilde{\Phi}_0 \right\rangle = \tilde{F}_{ab}^N - \delta_{ab}\tilde{F}_{ii}^N - \left\langle \tilde{a}\tilde{i} \parallel \tilde{b}\tilde{i} \right\rangle \\ &= \tilde{F}_{ab}^{N-i} - \delta_{ab}\tilde{F}_{ii}^{N-i}, \end{aligned}$$

In the above expression we employ the tilde symbol to indicate quantities calculated in the orbitals of the core ionized system. Upon diagonalization of the A block, we obtain the eigenvalues of the orbital-specific Fock operator $\hat{F}^{(N-i)}$, shifted by $\tilde{F}_{ii}^{N-i}$, which can be recognized as the negative of the core ionization energy, calculated in the frozen orbitals of the *core ionized* system, contrary to Koopmans' theorem, who uses the frozen orbitals of the parent system. It is corrected by rather using the ionization energy obtained by ΔSCF.

2.3 Projection analysis

In order to elucidate the electronic structure of the title species as well as to assign the simulated core excitation spectra we have performed projection analysis [93]. This method is akin to Mulliken population analysis, but the strong basis-set dependence of the latter method is avoided by expanding molecular orbitals in pre-calculated orbitals of the atoms constituting the molecule

$$|\psi_i\rangle = \sum_{Aj} \left|\psi_j^A\right\rangle c_{ji}^A + \left|\psi_i^{\text{pol}}\right\rangle, \tag{5}$$

where indices A and j refer to atoms and atomic orbitals (AOs), respectively. Charges and populations of atoms in the molecule are subsequently calculated in analogous manner to Mulliken

population analysis, but starting from molecular orbitals given as linear combinations of true and well-defined atomic orbitals, rather than in terms of atom-centered basis functions. The atoms are calculated in their proper basis and by default in their ground state configuration, either by average-of-configuration at the HF level or by using fractional occupation at the DFT level. In order to make the projection analysis chemically meaningful, the expansion in Eq. (5) is normally limited to AOs occupied in the atomic ground state configuration. However, for the assignment of the calculated core excitation spectra these orbitals, in the case of uranium, were supplemented by selected improved virtual orbitals, as discussed in section 4.3. In either case, the selected set of AOs is not guaranteed to fully span a given molecular orbital. The orthogonal complement $\left|\psi_i^{\mathrm{pol}}\right\rangle$, which we denote the polarization contribution, can be eliminated using the Intrinsic Atomic Orbital scheme of Knizia[94].

3 Computational details

Reference geometries were optimized at the scalar-relativistic CCSD(T) level using the MOLPRO 09[95] package and numerical gradients. For uranium we employed a relativistic small core potential (ECP60MDF) with a (14s13p10d8f6g)/[6s6p5d4f3g] quadruple zeta level valence ANO basis set developed by Dolg and Cao[46], and the (11s6p3d2f)/[5s4p3d2f] aug-cc-pVTZ basis sets[96, 97] for oxygen and nitrogen.

All other calculations were carried out with the DIRAC code [98] and are, unless otherwise stated, based on the 4-component Dirac-Coulomb Hamiltonian using the simple Coulombic correction [99] to avoid the explicit calculation of two-electron integrals involving the small components only. For uranium we employed the dyall.v3z basis set [100] (large component 33s29p20d13f4g2h) and for oxygen and nitrogen the cc-pVTZ basis set [96] (large components 10s5p2d1f). For MP2 calculations we switched to the slightly larger dyall.ae3z basis (large component 33s29p20d13f7g3h) for uranium. All basis sets were uncontracted and the small components generated by restricted kinetic balance. A finite nucleus model in the form of a Gaussian charge distribution was employed [101].

Uranium $2p$ ionization energies were calculated by ΔSCF calculations [59], both at the Kramers-restricted Hartree-Fock and Kohn-Sham level, the latter using the BLYP [102–104], B3LYP [105, 106], PBE [107], PBE0 [108], and CAM-B3LYP [109] functionals. Convergence of the core excited states was straightforward using initial reordering of orbitals followed by selection of orbitals based on overlap with starting orbitals during the SCF cycles.

The uranium L_3 edge XANES spectrum of the selected molecules was simulated by REW-TDDFT, CPP and STEX calculations, the former two using the CAM-B3LYP [109] functional. Transition moments have been calculated within the electric dipole approximation, more specifically in the length gauge, that is, as integrals over the electric dipole operator. The nature of the excitations was determined from the excitation amplitudes combined with Mulliken and projection analysis [93] of the involved molecular orbitals. In the REW-TDDFT and STEX calculations finite linewidths of the individual peaks were introduced by Lorentzian functions of half-width at half-maximum (HWHM) $\gamma = 0.0367\ E_h$ ($\sim$ 1eV). The same value of γ was taken as damping parameter in the CPP calculations.

4 Results and discussions

4.1 Molecular and electronic structures

Prior to the calculation of core ionization and excitation energies we optimized the geometries of the title species and investigated their electronic structures by projection analysis[93]. In Table 2 we report our calculated bond lengths for the isoelectronic series together with selected literature values. Wei *et al.* [23] reported bond lengths for NUO^+ and UN_2 calculated at the CCSD(T) level using the aug-cc-pVTZ basis set [96] for the ligands. For uranium the authors employed the rela-

tivistic small core potential ECP60MWB with the accompanying (12s11p10d8f)/[8s7p6d4f] valence basis, although it was developed for SCF calculations.[49] Jackson *et al.* [26] reported bond distances for UO_2^{2+} with the same computational setup, except that they added two g functions to the valence basis. Switching to the larger segmented valence basis set (14s13p10d8f6g)/[10s9p5d4f3g] developed by Cao and co-workers [110, 111] and further augmentation by h and i functions was found to have only a small effect on calculated bond lengths. More recently, Tu *et al.* reported bond lengths for the entire isoelectronic series with basically the same computational setup.[55] They reproduce the uranyl bond length reported by Jackson *et al.* [26], and get slightly shorter bond distances than reported by Wei *et al.* [23] for the other species. We have optimized bond lengths for the isoelectronic species using the more recent ECP60MDF core potential with the accompanying valence basis[46] and interestingly get somewhat longer bond lengths, closer to those reported by Gagliardi and Roos [48] at the CASPT2 level with ANO basis sets. Particularly noteworthy is that the U-N bond in the nitridooxouranium cation is shorter than the U-O bond, although experiment suggest that that the former is weaker than the latter (bond dissociation energies BDE[OU^+-N] = 4.44±1.27 eV *vs.* BDE[NU^+-O] = 7.66±1.70 eV).[31]

	Bond	CCSD(T)[pw]	CCSD(T)	CCSD(T)[55]	CASPT2[48]	PBE[34]
UO_2^{2+}	U-O	1.704	1.6898[26]	1.689	1.705	
OUN^+	U-O	1.748	1.743[23]	1.731	1.746	1.761
	U-N	1.696	1.703[23]	1.681	1.695	1.698
UN_2	U-N	1.736	1.743[23]	1.731	1.735	1.739

Table 2: *Calculated bond lengths (in Å) for the title species.*

We have also investigated the electronic structure of the title compounds by projection analysis[93] at the HF level using the pre-calculated atomic orbitals occupied in the electronic ground state of the constituent atoms. Polarization contributions have been eliminated by polarizing the atomic orbitals in the molecule according to the Intrinsic Atomic Orbital scheme of Knizia[94], yet conserving overlap between atomic orbitals on different centers. The charge and electronic configuration of uranium in the three molecules are given in Table 3. Concerning the electronic configurations, one in particular notes the 6*p*-hole [112], primarily arising from overlap between the $6p_{3/2}$ orbital with the ligands, and which is basically identical for the three species. The calculated atomic charges, which do not suffer from the strong basis set dependence of Mulliken charges, are far from the formal oxidation state +VI of uranium in these molecules, in agreement with previous theoretical and experimental studies.[113] The uranium charge furthermore reduces according to the total molecular charge, as expected. The ligand charge is -0.42*e* and in -0.73*e* in UO_2^{2+} and UN_2, respectively. In NUO^+ the charge on oxygen and nitrogen is -0.63*e* and -0.49*e*, respectively. The calculated dipole moment of $NUO^+$is -1.43 D, when the uranium atom is placed at the origin with the nitrogen atom along the positive axis. Interestingly, for certain initial start guesses the HF SCF procedure converges to a solution 0.2 E_h higher in energy and with atomic charges very slightly modified (Q_U=+2.16*e*, Q_O=-0.70*e*, Q_N= -0.45*e*), but enough to switch the sign of the calculated dipole moment (+1.55 D).

Molecule	Q_U	Atomic configuration
UO_2^{2+}	+2.84	$5f^{2.26}6p^{5.67}6d^{1.20}7s^{0.04}$
NUO^+	+2.12	$5f^{2.52}6p^{5.67}6d^{1.60}7s^{0.10}$
UN_2	+1.45	$5f^{2.68}6p^{5.66}6d^{2.01}7s^{0.23}$

Table 3: *Charge and electronic configuration of uranium in the title compounds obtained by projection analysis at the HF level.*

Canonical orbitals are quite suitable for the description of electron detachment and excitation processes, such as XPS and XAS, respectively. However, in order to "see" chemical bonds one needs to rotate the occupied molecular orbitals to form localized ones [114, 115], although

	ω	$\langle\varepsilon\rangle$	$U6p_{3/2}$	$U5f_{5/2}$	$U5f_{7/2}$	$U6d_{3/2}$	$U6d_{5/2}$	$U7s_{1/2}$	X	$X2s_{1/2}$	$X2p_{1/2}$	$X2p_{3/2}$
UO_2^{2+}	1/2	-1.487	0.09	0.19	0.18	0.08	0.08	0.00	O	0.10	0.34	0.88
	1/2	-1.078	0.00	0.10	0.12	0.12	0.09	0.00	O	0.00	1.09	0.43
	3/2	-1.075	0.00	0.07	0.16	0.05	0.16	0.00	O	0.00	0.00	1.52
NUO^+	1/2	-1.147	0.06	0.13	0.12	0.09	0.08	0.00	O	0.12	0.35	0.98
	1/2	-0.790	0.00	0.08	0.10	0.11	0.09	0.00	O	0.00	1.16	0.43
	3/2	-0.787	0.00	0.06	0.13	0.04	0.16	0.00	O	0.00	0.00	1.59
	1/2	-1.146	0.19	0.28	0.20	0.11	0.07	0.01	N	0.02	0.23	0.76
	1/2	-0.689	0.01	0.13	0.19	0.20	0.17	0.00	N	0.00	0.94	0.31
	3/2	-0.683	0.01	0.12	0.23	0.09	0.28	0.00	N	0.00	0.00	1.24
UN_2	1/2	-0.826	0.16	0.19	0.16	0.10	0.09	0.03	O	0.03	0.31	0.81
	1/2	-0.427	0.00	0.12	0.14	0.21	0.16	0.00	O	0.00	0.96	0.38
	3/2	-0.425	0.00	0.09	0.19	0.08	0.28	0.00	O	0.00	0.00	1.33

Table 4: *Projection analysis of Pipek-Mezey localized bonding orbitals in the title compounds at the HF level. $\langle\varepsilon\rangle$ refers to the expectation value (in E_h) of the converged Fock operator. X refers to the ligand.*

there is no unique localization criterion. In Table 4 we present a projection analysis of bonding orbitals obtained by Pipek-Mezey localization [116]. The bonding orbitals are identificed as localized molecular orbitals with significant contributions from both the uranium center and a (single) ligand. Approximate orbital eigenvalues have been calculated as expectation values of the converged Fock operator. For each ligand we find three such bonding orbitals, of which two are almost degenerate and with $\omega = 1/2$ and $3/2$, respectively. Based on our analysis we conclude that each ligand is bound to the central uranium atom by triple (σ,π) bonds, where the π bond has been split by spin-orbit interaction into $\pi_{1/2}$ and $\pi_{3/2}$, and where the metal center contributes *df* hybrid atomic orbitals.

4.2 Uranium *2p* binding energy

In table 5 we report relaxation Δ_{relax} and correlation Δ_{corr} contributions to the uranium *2p* ionization energies of the title species, for uranium using the dyall.ae3z basis set which include correlation functions for all occupied orbitals. The calculations are based on the default Hamiltonian of the DIRAC package, that is, the 4-component relativistic Dirac-Coulomb Hamiltonian with a simple Coulomb correction [99], thus avoiding the calculations of two-electron integrals $(SS|SS)$ containing small component basis functions only. At the HF level the uranium *2p* orbitals are split by 3838 eV due to spin-orbit interaction, and the $2p_{3/2}$ orbital further split by a mere 0.3 eV due to the molecular field. As illustrated by figure 1, the ΔHF uranium *2p* binding energies are a linear function, all with slope 13.4 eV/e, of the atomic charges reported in table 3, thus demonstrating the chemical shift of X-ray photoelectron spectroscopy [117, 118] as well as the usefulness of the atomic charges obtained from projection analysis.

Method	UO_2^{2+}			OUN^+			UN_2		
	$2p^{-1}_{1/2,1/2}$	$2p^{-1}_{3/2,1/2}$	$2p^{-1}_{3/2,3/2}$	$2p^{-1}_{1/2,1/2}$	$2p^{-1}_{3/2,1/2}$	$2p^{-1}_{3/2,3/2}$	$2p^{-1}_{1/2,1/2}$	$2p^{-1}_{3/2,1/2}$	$2p^{-1}_{3/2,3/2}$
Koopmans	21165.33	17321.80	17321.74	21155.86	17312.25	17312.32	21147.87	17304.32	17304.24
ΔHF	21094.94	17257.20	17257.31	21084.79	17247.02	17247.14	21076.27	17238.48	17238.61
ΔMP2	21089.94	17251.82	17251.55	21079.99	17241.85	17241.60	21069.13	17231.16	17230.89
Δ_{relax}	-70.40	-64.60	-64.43	-71.07	-65.23	-65.18	-71.61	-65.84	-65.63
Δ_{corr}	-5.00	-5.38	-5.76	-4.80	-5.17	-5.54	-7.14	-7.32	-7.72

Table 5: *Ionization energies (in eV) obtained with dyall.ae3z basis set for uranium.*

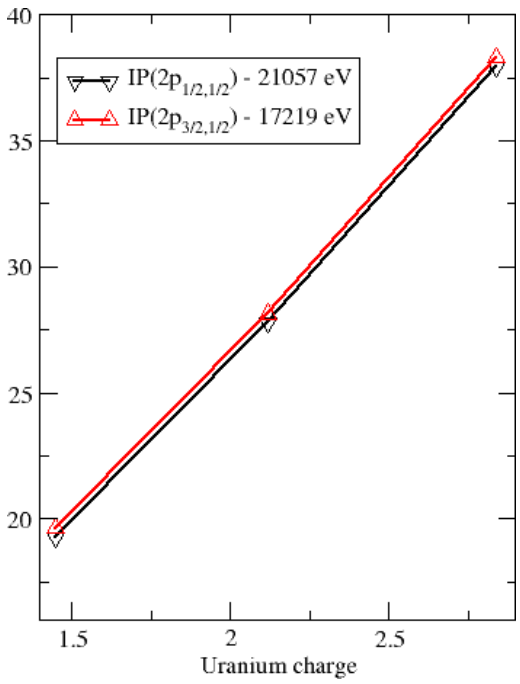

Figure 1: *Shifted ΔHF uranium 2p ionization energies of the title species (in eV) as a function of the uranium charge (in a.u.) from projection analysis.*

We have defined Δ_{corr} as the difference between the ionization energy (IP) obtained at the ΔMP2 and ΔHF level, that is,

$$\Delta_{corr} = IP\,(\Delta\text{MP2}\,) - IP\,(\Delta\text{HF}\,)\,,$$

but it should be emphasized that due to the non-canonical nature of the orbitals of the core ionized states, there will be non-zero T_1 contributions to the MP2 energy, that are more properly associated with relaxation (see Eq.(1)). However, these contributions are negligible in the calculations reported in Table 5, as will be discussed and demonstrated below. Table 5 shows that the correlation contribution Δ_{corr} is an order of magnitude smaller than the relaxation contribution Δ_{relax} and that the Koopmans estimate gives errors on the order of 75 eV. What is striking, though, is that the correlation contribution has the *same* sign as the relaxation contribution, that is, it is *negative*. If we consider the canonical MP2 energy expression

$$E^{MP2} = \sum_{i<j} e_{ij}; \quad e_{ij} = \sum_{a<b} \frac{|\langle ij\,||\,ab\rangle|^2}{\varepsilon_i + \varepsilon_j - \varepsilon_a - \varepsilon_b},$$

with N_o occupied and N_v virtual orbitals for the parent state, then the core-ionized state has $(N_o - 1)$ fewer pair energies e_{ij}, all of them negative in the parent state. In addition, the remaining pair energies has N_v new contributions containing the now virtual core orbital, such that denominators may be zero or even positive. Indelicato and co-workers[119–121], in the framework of many-body perturbation theory, makes a distinction between contributions to the ionization energy for which $|\varepsilon_i + \varepsilon_j| > |\varepsilon_h|$, where ε_h is the energy of the virtual core orbital, say b, and contributions for which $|\varepsilon_i + \varepsilon_j| < |\varepsilon_h|$ and refer to them core-core and Auger effects, respectively. Core-core contributions only occur if there are core orbitals lower in energy than the ionized one. The denominator is generally negative, but may change sign if the second virtual orbital, say a is bound, which are precisely the orbitals associated with pre-edge structure in X-ray absorption

spectroscopy. The denominator of Auger effect contributions, on the other hand, starts off positive with increasing energy of the second virtual orbital, but eventually become negative for sufficiently high-lying virtuals. Such contributions were observed by Nooijen and Bartlett [122] to lead to convergence problems in coupled-cluster calculations of core-ionized states and were therefore ignored. In the present non-canonical MP2 calculations we do not make a distinction between Auger and core-core contributions, but simply monitor contributions to the pair correlation energy of positive sign. For the $1a_1$ ionization energy of water the total contribution is quite small (0.13 eV), whereas we obtain 3.43 eV for the uranium $2p_{3/2,3/2}$ ionization of uranyl.

Molecule	IP	Orbital set	Δ_{relax}	Δ_{corr}	$\Delta_{corr}(T_1)$	$\Delta_{corr}(T_2)$
H_2O	$1a_1$	relaxed	-20.51	0.92	-0.17	1.08
		frozen	0.00	-34.58	-35.50	0.92
UO_2^{2+}	$2p_{3/2,3/2}$	relaxed	-64.54	-5.17	-0.28	-4.89
		frozen	0.06	-103.91	-106.08	2.17

Table 6: Relaxation and correlation contributions (in eV) to core ionization energies of water and uranyl. See text for further details.

The above discussion confirms the expectation that the correlation contribution should be positive. However, a negative contribution, arising from a strong coupling of correlation and relaxation, can not be excluded. To investigate this, we carried out non-canonical MP2 calculations on core-ionized uranyl as well as water using the molecular orbitals of the parent state. The results are shown in table 6. Using the orbitals of the parent state (denoted "frozen" in the table) the relaxation contribution Δ_{relax} is by definition zero, to within numerical noise. The correlation contribution Δ_{corr}, on the other hand, becomes negative for both water and uranyl. However, when decomposing Δ_{corr} further into T_1 and T_2 contributions, according the the non-canonical MP2 expression of Eq. (1), one observes that the T_1- contribution, which can be associated with relaxation, is completely dominating. For water the T_2- contribution $\Delta_{corr}(T_2)$ remains positive and is basically the same as when using relaxed orbitals. For uranyl, on the other, hand the T_2 - contribution using frozen orbitals is positive, leading us to conclude that the negative correlation contribution obtained with the relaxed orbitals is indeed due to a strong coupling of correlation and relaxation.

Method	UO_2^{2+}			OUN^+			UN_2		
	$2p^{-1}_{1/2,1/2}$	$2p^{-1}_{3/2,1/2}$	$2p^{-1}_{3/2,3/2}$	$2p^{-1}_{1/2,1/2}$	$2p^{-1}_{3/2,1/2}$	$2p^{-1}_{3/2,3/2}$	$2p^{-1}_{1/2,1/2}$	$2p^{-1}_{3/2,1/2}$	$2p^{-1}_{3/2,3/2}$
ΔHF	21095.41	17257.59	17257.71	21085.26	17247.41	17247.54	21076.74	17238.87	17239.01
ΔΔDOSSSS	-18.01	-5.86	-5.86	-18.00	-5.85	-5.86	-18.01	-5.86	-5.86
ΔΔGaunt	-108.73	-68.90	-68.90	-108.73	-68.91	-68.90	-108.74	-68.91	-68.91
ΔΔPBE	-14.41	-59.09	-59.02	-13.90	-58.58	-58.50	-13.53	-58.21	-58.13
ΔΔBLYP	-11.35	-57.03	-56.96	-10.84	-56.51	-56.44	-10.46	-56.12	-56.05
ΔΔPBE0	23.49	-15.91	-15.86	23.83	-15.57	-15.52	24.05	-15.35	-15.29
ΔΔB3LYP	17.89	-22.98	-22.92	18.25	-22.61	-22.55	18.52	-22.34	-22.28
ΔΔCAMB3LYP	18.82	-22.67	-22.62	19.14	-22.35	-22.29	19.37	-22.12	-22.06

Table 7: *Ionization energies (in eV) obtained using the dyall.v3z basis set for uranium.*

We now turn to the effect of extensions to the default Hamiltonian of the DIRAC package. In table 7 we report the effect of explicit inclusion of the $(SS|SS)$ class of integrals (ΔΔDOSSSS). Although the effect is sizable, causing a reduction of binding energies on the order of 18 and 6 eV for uranium $2p_{1/2}$ and $2p_{3/2}$ orbitals, respectively, it is constant for all three isoelectronic species, and

thus does not contribute to the chemical shift. Even more important is the effect of the inclusion of the Gaunt two-electron interaction, but again the chemical shift is not affected, and so we have ignored these both $(SS|SS)$ integrals and the Gaunt term in the subsequent calculations. In passing we note that the Gaunt term reduces the spin-orbit splitting of the uranium 2p manifold by about 40 eV, which makes sense, since the Gaunt term contains the spin-other-orbit interaction[45].

We have also investigated the performance of a selection of DFT functionals for the calculation of uranium 2p binding energies of the title species. These are reported in table 7 relative to the HF binding energies. To the extent that the difference between HF and DFT binding energies can be interpreted as pure correlation contributions, we note that these are significantly larger in magnitude than the correlation contributions extracted from the ΔMP2 calculations. It should be noted that the core ionized species have been calculated under Kramers restriction such that spin polarization, which is expected to reduce ionization energies, is missing. The GGA functionals PBE and BLYP reduce both uranium $2p_{1/2}$ and $2p_{3/2}$ binding energies, whereas the global hybrid functionals PBE0 and B3LYP, as well as the long-range corrected hybrid CAMB3LYP, decrease the $2p_{3/2}$ binding energies and increase the $2p_{1/2}$ ones. No DFT functional have a performance similar to MP2.

No experimental uranium L_2 or L_3 binding energies are available for the title species. The $2p_{1/2}$ and $2p_{3/2}$ binding energies of metallic uranium is 20948 and 17166 eV, respectively, relative to the Fermi level[123]. If we add the $(SS|SS)$ and Gaunt contributions as corrections, then the MP2 ionization energies for UN_2, in which uranium has the smallest charge, agree to within 10 eV with the cited experimental numbers. If we instead linearly extrapolate the MP2 ionization energies to zero uranium nuclear charge at the HF level and add the cited corrections, we underestimate the experimental numbers by about 30 eV.

4.3 Uranium L_3 edge XANES spectra

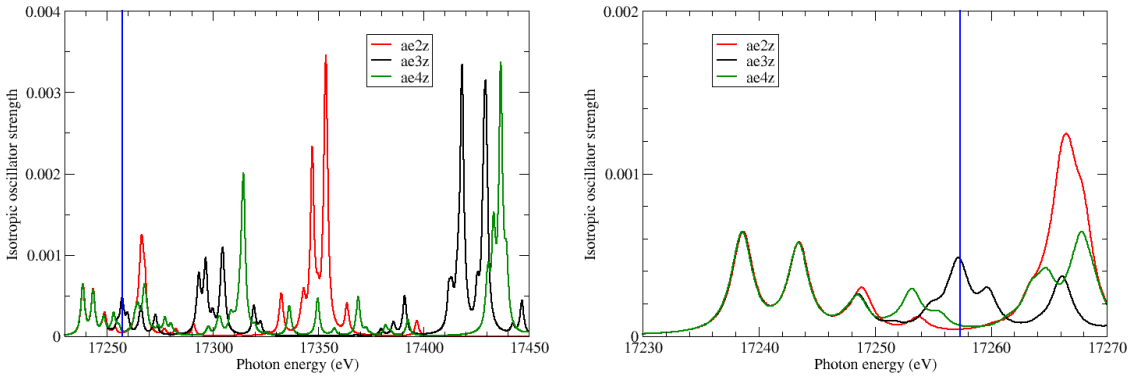

Figure 2: *(left)* UO_2^{2+} *uranium* L_3 *edge XANES spectra simulated by STEX using different basis sets and a Lorentzian broadening of* $\sim$ 1eV*. The vertical line indicates the ionization threshold obtained at the ΔHF level (the value changes less than 0.1 eV with the indicated basis sets). To the right a zoom of the pre-edge region.*

In this section we present and analyze simulated uranium L_3 edge XANES spectra of the title species. A good discussion of the electronic structure of actinyls has been given by Denning [124]. Here focus will be on the bound virtual orbitals. We start by considering the calculated uranium L_3 edge XANES spectrum for uranyl obtained by the STEX method. In the left panel of figure 2 we compare the spectra obtained with three different basis sets. These are local Gaussian basis sets which are not appropriate for the description of continuum states[125], as can be seen from the lack of any convergence of the spectra with respect to basis sets beyond the L_3 edge. Such

artifacts have been observed previously, and it was suggested by Ekström and Norman that the meaningful energy range of a simulated spectrum in a local basis can be ascertained by exponent scaling [126]. In the present case, a zoom into the pre-edge region of the spectrum, as shown in the right panel of figure 2 suggests that the spectrum is not fully converged for quasi-bound states in the vicinity of the ionization threshold. Convergence in this region would probably require a rather extensive set of diffuse functions. In the following we shall therefore focus on the first three peaks of the spectrum.

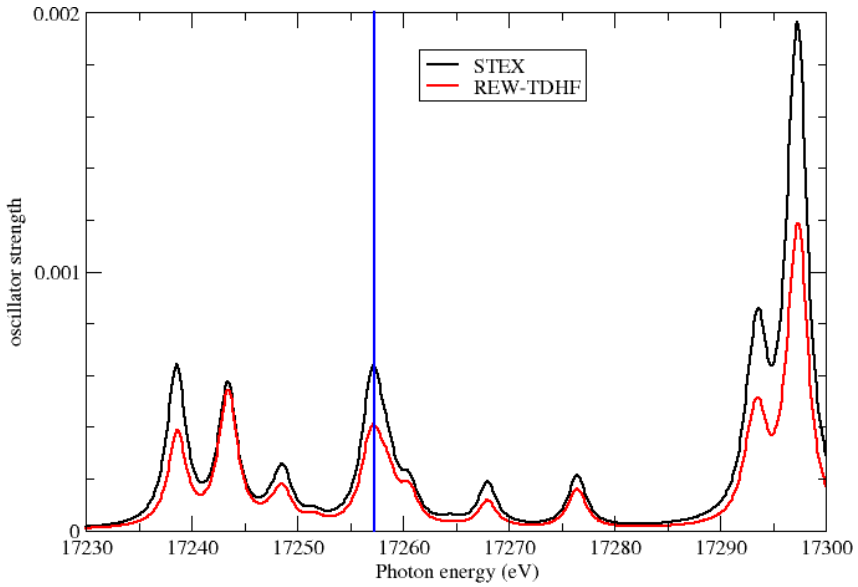

Figure 3: *Comparison of UO_2^{2+} uranium L_3 edge XANES spectra obtained by STEX and REW-TDHF, in both cases adding a Lorentzian broadening of* $\sim$ 1eV. *The REW-TDHF calculations has been carried out within the Tamm-Dancoff approximation and using the orbitals of the core ionized state. The vertical line indicates the ionization threshold obtained at the ΔHF level. The REW-TDHF and STEX excitation energies are both corrected by the difference between the ground state energy calculated in ground state and core ionized orbitals.*

We shall also compare the performance of the three different methods discussed in section 2.2. We start by demonstrating numerically that the STEX excitation energies can be obtained by using a REW-TDHF calculation within the Tamm-Dancoff approximation and using the orbitals of the core ionized state. In figure 3 the uranium L_3 edge XANES spectrum for uranyl calculated by the two methods is displayed. As discussed in section 2.2 both the STEX and the TDHF/TDA excitation energies has been corrected as

$$\hbar\omega_m \rightarrow \hbar\omega_m + E_0 - \tilde{E}_0$$

where E_0 and $\tilde{E}_0$ is the energy of the parent state calculated in the parent and core ionized orbitals, respectively. The same correction is applied to the oscillator strengths, Eq.(4). The excitation energies are indeed seen to match perfectly, whereas the REW-TDHF/TDA Lorentz-broadened oscillator strengths are systematically smaller than the STEX ones.

A direct comparison of STEX on the one hand and CPP and REW-TDDFT on the other hand is complicated by the fact that the latter spectra are significantly shifted with respect to the experimental L_3 edge due to the combined effect of missing orbital relaxation and self-interaction errors[127]. In order to align the spectra we have therefore considered the position of the L_3 ionization threshold within a linear response regime. We may consider the process of ionization as

Molecule	Estimated IP(U2$p_{3/2}$) in eV	$-\varepsilon_{2p_{3/2}}$(eV)
UO_2^{2+}	17104.31	17104.41
OUN^+	17095.03	17095.13
UN_2	17087.25	17087.34

Table 8: *Estimated ionization potential of uranium $2p_{3/2}$ orbital (in eV) based on excitation to a tight ghost function placed 100 a_0 away from uranium, compared to the negative orbital energy $-\varepsilon_{2p_{3/2}}$ (averaged over the m_j components). All results have been obtained with the CAMB3LYP functional.*

an extreme case of a charge-transfer excitation in which the separation between donor and acceptor tends towards infinity. Following the arguments of Dreuw *et al.*[128], it then becomes clear that the excitation energy reduces, for any DFT functional, to the energy difference between the acceptor and donor orbital. Since this excitation energy is also equal to the difference between the ionization potential of the donor and the electron affinity of the acceptor we are led to the conclusion that within TDDFT (and TDHF) the ionization threshold is *de facto* given by Koopmans' theorem, that is, as the negative of the donor orbital. We have tested this conclusion numerically by forcing an excitation from the selected core orbital to a remote tight ghost function placed 100 a_0 away from the uranium atom along the molecular axis and then subtracting the ghost orbital eigenvalue from the resulting excitation energy. The results are given in table 8 and clearly confirms the validity of our conclusion. On the other hand, it should be emphasize that the meaning of orbital eigenvalues is different in Hartree-Fock and exact Kohn-Sham theory.[129–131]

As a consequence we have shifted the excitation energies obtained with CPP and REW-TDDFT according to

$$\hbar\omega_m \rightarrow \hbar\omega_m + IP_i\,(\Delta HF) + \varepsilon_i^{KS} \tag{6}$$

From figures 4, 5 and 6 it is seen that these shifts, on the order of 150 eV, clearly bring the CPP and REW-TDDFT spectra into the same energy region as the STEX one. The CPP and REW-TDDFT spectra agree perfectly, as they should (cf. section 2.2); the slight deviation observed towards higher photon energies in figure 5 is simply due to an insufficient number of excitations calculated at the REW-TDDFT level. For uranyl the CPP and REW-TDDFT spectra are seen to match the STEX one very well, but the agreement deteriorates as the molecular charge is reduced along the isoelectronic series. For OUN^+we note in particular new pre-edge features with respect to STEX. It should be pointed out, however, that the uranium $2p_{3/2}$ natural width is 7.43 eV [132], although the experimental energy resolution can be reduced down to about 4 eV using partial fluorescence yield techniques[10, 133]. This still means that the above-mentioned pre-edge structures of the theoretical spectrum can not be resolved by present-day experiment.

Amongst the three methods STEX offers perhaps the most straightforward assignment of spectra. This is because XANES spectroscopy, in an orbital picture, probes bound virtual orbitals which, as discussed in section 2.2, has been optimized by calculating the core ionized state. As an illustration we may note that in the dyall.v3z basis an HF calculation on the uranyl ground state gives 41 bound virtual orbitals (Kramers pairs). whereas for OUN^+ this number is reduced to 15 and for UN_2 there are none. In contrast, the corresponding numbers for the uranium $2p_{3/2}$-ionized state are 46, 35 and 15, respectively. We have been able to carry out a detailed assignment of the STEX uranium L_3 XANES spectra using projection analysis[93]. For the ligands we have used the ground state orbitals. For uranium the ground state occupied orbitals were supplemented by the bound improved virtual orbitals generated by freezing the ground state orbitals and then

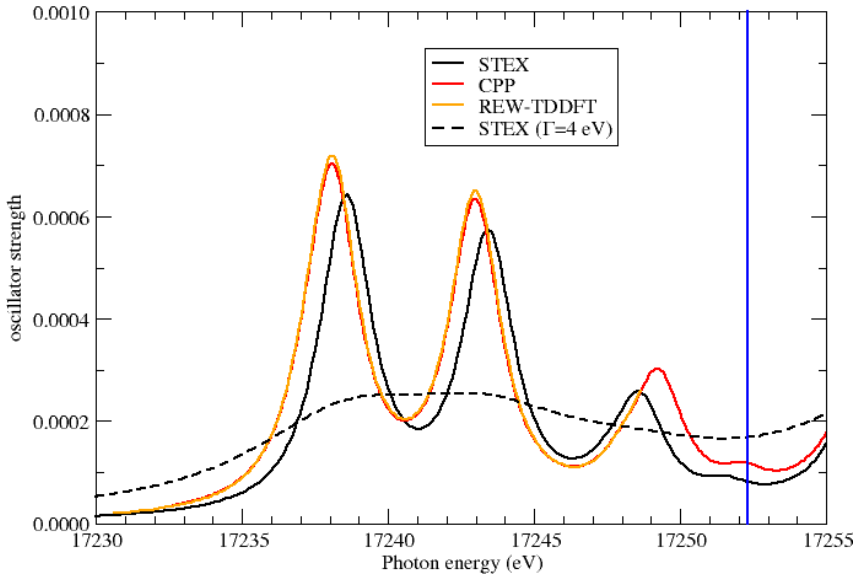

Figure 4: *UO_2^{2+} uranium L_3 edge XANES spectra simulated by STEX, CPP(CAM-B3LYP) and REW-TDDFT(CAM-B3LYP), including a Lorentzian broadening of* ~ 1 eV. *The two latter spectra have been shifted by 152.63 eV according to (6).*

recalculating the virtual orbitals for the $2p_{3/2}$- ionized state. The first peak of the uranyl STEX spectrum (cf. figure 4) is thereby found to be dominated by excitations to uranium 6d orbitals, but also a virtual orbitals of uranium 7s character. These virtual orbitals have essentially no ligand character. The second peak is assigned as excitations to virtual orbitals dominated by uranium 6d, but about 25 % ligand character. The third and final peak before the ionization threshold is dominated by excitations to uranium 7d orbitals. Moving to OUN^+ the molecular charge is reduced by one unit and the number of peaks before the ionization threshold to two; both are dominated by excitations to uranium 6d orbitals, but the second peak also has some ligand character (23 % nitrogen and 6% oxygen). Finally, for neutral UN_2 there is a single peak before the ionization threshold dominated by excitations to uranium 6d and with no ligand character. The same assignment basically carries over to the CPP and REW-TDDFT spectra, but with less precision since the virtual orbitals are less optimal. The extra features of the second peak of the OUN^+ spectrum (cf. figure 5) appears to be due to a larger splitting of the $\omega = 3/2$ and $\omega = 5/2$ components of the uranium $6d_{5/2}$ orbitals.

5 Conclusions and perspectives

In the present work we have studied the processes of ionization and excitation out of the uranium $2p_{3/2}$ orbital in the isoelectronic species UO_2^{2+}, OUN^+ and UN_2 at the 4-component relativistic level. Molecular geometries were reoptimized at the CCSD(T) level using small-core scalar relativistic pseudopotentials and correlation-consistent basis sets, and the electronic structure studied by projection analysis in localized orbitals. Using the extracted uranium atomic charges we find a perfectly linear chemical shift of uranium $2p_{3/2}$ ionization energies obtained by ΔHF. We confirm the failure of Koopmans' theorem for core ionization due to the dominance of relaxation contributions over correlation ones. More unexpected is that the correlation contribution Δ_{corr} is negative for all three species, meaning that the parent state has less correlation energy than the core ionized state. Our analysis suggests that this is due to a strong coupling of relaxation and correlation. Uranium $2p_{3/2}$ ionization energies calculated by ΔSCF using different DFT functionals do not agree very well with our ΔMP2 values, but this situation might improve by the introduction of

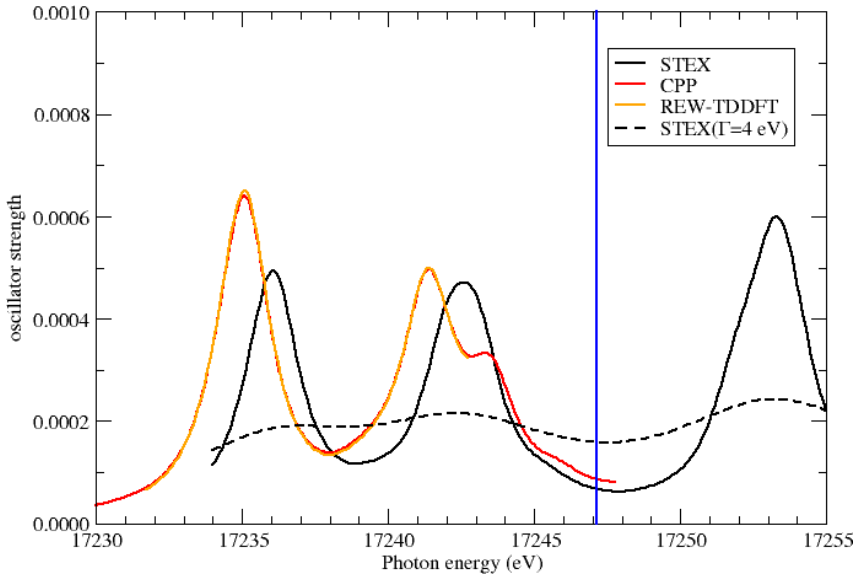

Figure 5: *OUN^+ uranium L_3 edge XANES spectra simulated by STEX, CPP(CAM-B3LYP) and REW-TDDFT(CAM-B3LYP), including a Lorentzian broadening of* ~ 1 eV. *The two latter spectra have been shifted by 151.73 eV according to (6).*

spin polarization in a Kramers unrestricted formalism.

To describe core excitations we have investigated three methods and shown how they are related. In particular, we show how STEX excitation energies, but not intensities, can be reproduced by TDHF calculations within the Tamm-Dancoff approximation. We also show that for the same Lorentz broadening REW-TDDFT and CPP give identical spectra. The CPP method has a certain ease of application in that the spectrum is directly simulated by scanning the desired frequency region, without any worry about the appropriate number of excitations to include. On the other hand, CPP lacks some flexibility in that spectra are only simulated for one specific damping parameter and would therefore have to be recalculated if another value was chosen. Although Koopmans' theorem fails for core excitations, it is the correct approximation of ionization potentials in the linear response regime, and this observation has allowed us to introduce shifts (cf. Eq (6)), on the order of 150 eV, to align REW-TDDFT and CPP uranium L_3 XANES spectra with the STEX ones. Since orbital relaxation dominates over electron correlation for core excitations, the ionization threshold of STEX spectra are in the vicinity of experimental ones. The interpretation of STEX spectra is furthermore more straightforward in that the virtual orbitals of the core ionized state are optimal. We accordingly obtain a detailed assignment of our calculated STEX spectra using projection analysis, notably with improved virtual orbitals of the uranium atom. On the other hand, it has been claimed (see for instance [134]) that REW-TDDFT (and thus CPP) gives better relative peak positions and intensities than STEX compared to experiment due to the inclusion of electron correlation. In the present work no direct comparison with experiment was made. In future work we plan to address this issue in detail. It should also be pointed out that the molecules in the present study are closed shell in their parent state, which is rather the exception in the domain of f-elements. As pointed out by Roemelt *et al.*[135], TDDFT (and therefore also CPP and STEX) has simply not enough parameters to handle the general open-shell case. A challenge for the future is therefore to develop cost-effective methods for the simulation of X-ray spectra of actinide species.

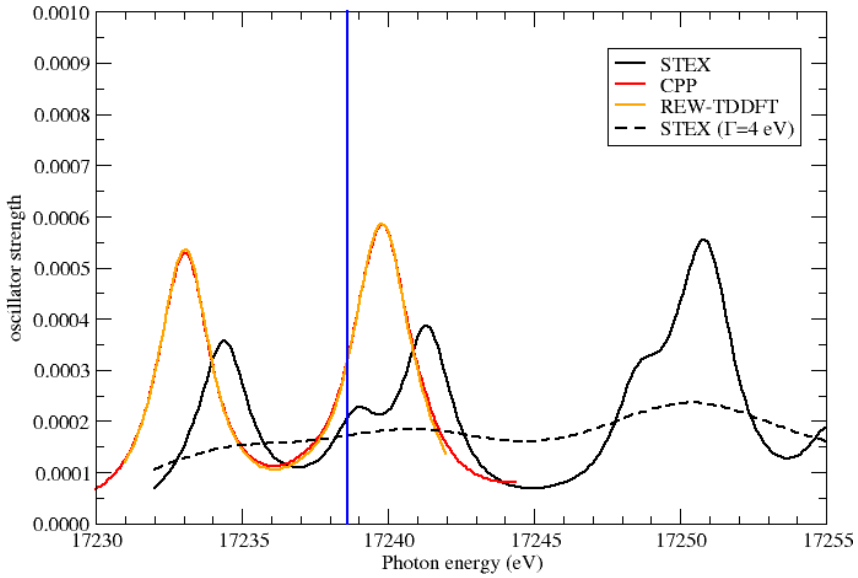

Figure 6: *UN_2 uranium L_3 edge XANES spectra simulated by STEX, CPP(CAM-B3LYP) and REW-TDDFT(CAM-B3LYP), including a Lorentzian broadening of* ~ 1 eV. *The two latter spectra have been shifted by 150.98 eV according to (6).*

Acknowledgements

TS and DM acknowledges financial support from the Indo-French Centre for the Promotion of Advanced Research (IFCPAR project No. 4705-3), including the PhD-grant for AS . Computing time from CALMIP (Calcul en Midi-Pyrenées) is gratefully acknowledged. TS would like to acknowledge helpful discussions with Paul Bagus (Denton) , Vincenzo Carravetta (Pisa), Ulf Ekström (Oslo), Eva Lindroth (Stockholm), Patrick Norman (Linköping) and Tonya Vitova (Karlsruhe). AKW acknowledges support of the National Science Foundation under Grant No. CHE-1362479. Computing support, in part, was provided by the Computing and Information Technology Center at the University of North Texas. Support is provided by the U.S. Department of Energy (DOE) for the Center for Advanced Scientific Computing and Modeling (CASCaM) at the University of North Texas. AKW and CS acknowledge support from the Global Research Experiences, Exchange, and Training (GREET) program, a program of the American Chemical Society. We are happy to dedicate this paper to Evert Jan Baerends on the occasion of his 70th birthday.

References

[1] Joel Selbin and J. D. Ortego. Chemistry of uranium (V). *Chem. Rev.*, 69(5):657–671, 1969. doi: 10.1021/cr60261a004. URL http://dx.doi.org/10.1021/cr60261a004.

[2] Kurt A. Kraus, Frederick. Nelson, and Gordon L. Johnson. Chemistry of Aqueous Uranium(V) Solutions. I. Preparation and Properties. Analogy between Uranium(V), Neptunium(V) and Plutonium(V). *J. Am. Chem. Soc.*, 71(7):2510–2517, 1949. doi: 10.1021/ja01175a079. URL http://dx.doi.org/10.1021/ja01175a079.

[3] Kurt A. Kraus and Frederick. Nelson. Chemistry of Aqueous Uranium(V) Solutions. II. Reaction of Uranium Pentachloride with Water. Thermodynamic Stability of UO2+. Potential of U(IV)/(V), U(IV)/(VI) and U(V)/(VI) Couples. *J. Am. Chem. Soc*, 71(7):2517–2522, 1949. doi: 10.1021/ja01175a080. URL http://dx.doi.org/10.1021/ja01175a080.

[4] Frederick Nelson and Kurt A. Kraus. Chemistry of Aqueous Uranium (V) Solutions. III. The Uranium (IV)-(V)-(VI) Equilibrium in Perchlorate and Chloride Solutions. *J. Am. Chem. Soc.*, 73(5):2157–2161, 1951. doi: 10.1021/ja01149a071. URL http://dx.doi.org/10.1021/ja01149a071.

[5] Francis R. Livens, Mark J. Jones, Amanda J. Hynes, John M. Charnock, J.Fred W. Mosselmans, Christoph Hennig, Helen Steele, David Collison, David J. Vaughan, Richard A.D. Pattrick, Wendy A. Reed, and Lesley N. Moyes. X-ray absorption spectroscopy studies of reactions of technetium, uranium and neptunium with mackinawite. *J. Environ. Radioact.*, 74(1-3):211 – 219, 2004. ISSN 0265-931X. doi: 10.1016/j.jenvrad.2004.01.012. URL http://www.sciencedirect.com/science/article/pii/S0265931X04000177. Papers from the International Conference on Radioactivity in the Environment, Monaco, 1-5 September 2002.

[6] E.H. Bailey, J.F.W. Mosselmans, and P.F. Schofield. Uranyl-citrate speciation in acidic aqueous solutions — an XAS study between 25 and 200 °C. *Chem. Geol.*, 216(1-2):1 – 16, 2005. ISSN 0009-2541. doi: 10.1016/j.chemgeo.2004.10.011. URL http://www.sciencedirect.com/science/article/pii/S0009254104004553.

[7] Melissa A. Denecke. Actinide speciation using X-ray absorption fine structure spectroscopy . *Coord. Chem. Rev.*, 250(7-8):730 – 754, 2006. doi: 10.1016/j.ccr.2005.09.004. URL http://www.sciencedirect.com/science/article/pii/S0010854505002122.

[8] Nebebech Belai, Mark Frisch, Eugene S. Ilton, Bruce Ravel, and Christopher L. Cahill. Pentavalent Uranium Oxide via Reduction of $[UO_2]^{2+}$ Under Hydrothermal Reaction Conditions. *Inorg. Chem.*, 47(21):10135–10140, 2008. doi: 10.1021/ic801534m. URL http://dx.doi.org/10.1021/ic801534m. PMID: 18842038.

[9] Clara Fillaux, Dominique Guillaumont, Jean-Claude Berthet, Roy Copping, David K. Shuh, Tolek Tyliszczak, and Christophe Den Auwer. Investigating the electronic structure and bonding in uranyl compounds by combining NEXAFS spectroscopy and quantum chemistry. *Phys. Chem. Chem. Phys.*, 12:14253–14262, 2010. doi: 10.1039/C0CP00386G. URL http://dx.doi.org/10.1039/C0CP00386G.

[10] T. Vitova, K. O. Kvashnina, G. Nocton, G. Sukharina, M. A. Denecke, S. M. Butorin, M. Mazzanti, R. Caciuffo, A. Soldatov, T. Behrends, and H. Geckeis. High energy resolution x-ray absorption spectroscopy study of uranium in varying valence states. *Phys. Rev. B*, 82: 235118, Dec 2010. doi: 10.1103/PhysRevB.82.235118. URL http://link.aps.org/doi/10.1103/PhysRevB.82.235118.

[11] Astrid Barkleit, Harald Foerstendorf, Bo Li, Andre Rossberg, Henry Moll, and Gert Bernhard. Coordination of uranium(VI) with functional groups of bacterial lipopolysaccharide

studied by EXAFS and FT-IR spectroscopy. *Dalton Trans.*, 40:9868–9876, 2011. doi: 10.1039/C1DT10546A. URL http://dx.doi.org/10.1039/C1DT10546A.

[12] Raymond Atta-Fynn, Donald F. Johnson, Eric J. Bylaska, Eugene S. Ilton, Gregory K. Schenter, and Wibe A. de Jong. Structure and Hydrolysis of the U(IV), U(V), and U(VI) Aqua Ions from Ab Initio Molecular Simulations. *Inorg. Chem.*, 51(5):3016–3024, 2012. doi: 10.1021/ic202338z. URL http://dx.doi.org/10.1021/ic202338z. PMID: 22339109.

[13] Frederic Poineau, CharlesB. Yeamans, G.W.C. Silva, GaryS. Cerefice, AlfredP. Sattelberger, and KennethR. Czerwinski. X-ray absorption fine structure spectroscopic study of uranium nitrides. *J. Radioanal. Nucl. Chem.*, 292(3):989–994, 2012. ISSN 0236-5731. doi: 10.1007/s10967-011-1551-7. URL http://dx.doi.org/10.1007/s10967-011-1551-7.

[14] Aurora Walshe, Tim Prußmann, Tonya Vitova, and Robert J. Baker. An EXAFS and HR-XANES study of the uranyl peroxides [UO2(η^2-O_2)(H_2O)$_2$]·nH_2O (n = 0, 2) and uranyl (oxy)hydroxide [(UO_2)$_4$O(OH)$_6$]·6H2$_2$O. *Dalton Trans.*, 43:4400–4407, 2014. doi: 10.1039/C3DT52437J. URL http://dx.doi.org/10.1039/C3DT52437J.

[15] Connie J. Nelin, Paul S. Bagus, and Eugene S. Ilton. Theoretical analysis of the U L_3-edge NEXAFS in U oxides. *RSC Adv.*, 4:7148–7153, 2014. doi: 10.1039/C3RA46738D. URL http://dx.doi.org/10.1039/C3RA46738D.

[16] Glen D. Lawrence, Kamalkumar S. Patel, and Aviva Nusbaum. Uranium toxicity and chelation therapy. *Pure Appl. Chem*, 6:1105–1110, 2014. doi: 10.1515/pac-2014-01. URL http://dx.doi.org/10.1515/pac-2014-01.

[17] Attila Kovács, Rudy J. M. Konings, John K. Gibson, Ivan Infante, and Laura Gagliardi. Quantum Chemical Calculations and Experimental Investigations of Molecular Actinide Oxides. *Chem. Rev.*, 115(4):1725–1759, 2015. doi: 10.1021/cr500426s.

[18] Virgil E. Jackson, Keith E. Gutowski, and David A. Dixon. Density Functional Theory Study of the Complexation of the Uranyl Dication with Anionic Phosphate Ligands with and without Water Molecules. *J. Phys. Chem. A*, 117(36):8939–8957, 2013. doi: 10.1021/jp405470k. URL http://dx.doi.org/10.1021/jp405470k. PMID: 23905705.

[19] Valérie Vallet, Ulf Wahlgren, and Ingmar Grenthe. Probing the Nature of Chemical Bonding in Uranyl(VI) Complexes with Quantum Chemical Methods. *J. Phys. Chem. A*, 116 (50):12373–12380, 2012. doi: 10.1021/jp3091123. URL http://dx.doi.org/10.1021/jp3091123. PMID: 23151258.

[20] Pawel Tecmer, Radovan Bast, Kenneth Ruud, and Lucas Visscher. Charge-Transfer Excitations in Uranyl Tetrachloride ($[UO_2Cl_4]^{2-}$): How Reliable are Electronic Spectra from Relativistic Time-Dependent Density Functional Theory? *J. Phys. Chem. A*, 116(27): 7397–7404, 2012. doi: 10.1021/jp3011266. URL http://dx.doi.org/10.1021/jp3011266. PMID: 22686595.

[21] Daniel Rios, George Schoendorff, Michael J. Van Stipdonk, Mark S. Gordon, Theresa L. Windus, John K. Gibson, and Wibe A. de Jong. Roles of Acetone and Diacetone Alcohol in Coordination and Dissociation Reactions of Uranyl Complexes. *Inorg. Chem.*, 51(23):12768–12775, 2012. doi: 10.1021/ic3015964. URL http://dx.doi.org/10.1021/ic3015964. PMID: 23146003.

[22] Boris B. Averkiev, Manjeera Mantina, Rosendo Valero, Ivan Infante, Attila Kovacs, DonaldG. Truhlar, and Laura Gagliardi. How accurate are electronic structure methods for actinoid chemistry? *Theor. Chem. Acc.*, 129(3-5):657–666, 2011. ISSN 1432-881X. doi: 10.1007/s00214-011-0913-0. URL http://dx.doi.org/10.1007/s00214-011-0913-0.

[23] Fan Wei, Guoshi Wu, W.H.Eugen Schwarz, and Jun Li. Geometries, electronic structures, and excited states of UN2, NUO^+, and UO_2^{2+}: a combined CCSD(T), RAS/CASPT2 and TDDFT study. *Theor. Chem. Acc.*, 129(3-5):467–481, 2011. doi: 10.1007/s00214-010-0885-5. URL http://dx.doi.org/10.1007/s00214-010-0885-5.

[24] Fernando Ruipérez, Cécile Danilo, Florent Réal, Jean-Pierre Flament, Valérie Vallet, and Ulf Wahlgren. An ab Initio Theoretical Study of the Electronic Structure of UO_2^+ and $[UO_2(CO_3)_3]^{5-}$. *J. Phys. Chem. A*, 113(8):1420–1428, 2009. doi: 10.1021/jp809108h. URL http://dx.doi.org/10.1021/jp809108h.

[25] Florent Réal, André Severo Pereira Gomes, Lucas Visscher, Valérie Vallet, and Ephraim Eliav. Benchmarking Electronic Structure Calculations on the Bare UO_2^{2+} Ion: How Different are Single and Multireference Electron Correlation Methods? *J. Phys. Chem. A*, 113(45):12504–12511, 2009. doi: 10.1021/jp903758c. URL http://dx.doi.org/10.1021/jp903758c. PMID: 19888775.

[26] Virgil E. Jackson, Raluca Craciun, David A. Dixon, Kirk A. Peterson, and Wibe A. de Jong. Prediction of Vibrational Frequencies of UO_2^{2+} at the CCSD(T) Level. *J. Phys. Chem. A*, 112(17):4095–4099, 2008. doi: 10.1021/jp710334b.

[27] Jason L. Sonnenberg, P. Jeffrey Hay, Richard L. Martin, , and Bruce E. Bursten. Theoretical Investigations of Uranyl-Ligand Bonding: Four- and Five-Coordinate Uranyl Cyanide, Isocyanide, Carbonyl, and Hydroxide Complexes. *Inorg. Chem.*, 44(7):2255–2262, 2005. doi: 10.1021/ic048567u. URL http://dx.doi.org/10.1021/ic048567u. PMID: 15792460.

[28] Kristine Pierloot and Els van Besien. Electronic structure and spectrum of UO_2^{2+} and $UO_2Cl_4^{2-}$. *J. Chem. Phys.*, 123(20):204309, 2005. doi: http://dx.doi.org/10.1063/1.2121608. URL http://scitation.aip.org/content/aip/journal/jcp/123/20/10.1063/1.2121608.

[29] Nikolas Kaltsoyannis. Computational Study of Analogues of the Uranyl Ion Containing the –NUN– Unit: Density Functional Theory Calculations on UO_2^{2+}, UON^+, UN_2, $UO(NPH_3)^{3+}$, $U(NPH_3)_2^{4+}$, $[UCl_4NPR_{32}]$ (R = H, Me), and $[UOCl_4NP(C_6H_5)_3]^-$. *Inorganic Chemistry*, 39(26):6009–6017, 2000. doi: 10.1021/ic000891b.

[30] J. Simon Craw, Mark A. Vincent, Ian H. Hillier, and Andrew L. Wallwork. Ab Initio Quantum Chemical Calculations on Uranyl UO_2^{2+}, Plutonyl PuO_2^{2+}, and Their Nitrates and Sulfates. *J. Phys. Chem.*, 99(25):10181–10185, 1995. doi: 10.1021/j100025a019. URL http://dx.doi.org/10.1021/j100025a019.

[31] Christoph Heinemann and Helmut Schwarz. NUO^+, a New Species Isoelectronic to the Uranyl Dication UO_2^{2+}. *Chem. Eur. J.*, 1(1):7–11, 1995. ISSN 1521-3765. doi: 10.1002/chem.19950010105. URL http://dx.doi.org/10.1002/chem.19950010105.

[32] Pekka Pyykkö, Jian Li, and Nino Runeberg. Quasirelativistic Pseudopotential Study of Species Isoelectronic to Uranyl and the Equatorial Coordination of Uranyl. *J. Phys. Chem.*, 98(18):4809–4813, 1994. doi: 10.1021/j100069a007.

[33] Kristine Pierloot, Els van Besien, Erik van Lenthe, and Evert Jan Baerends. Electronic spectrum of UO_2^{2+} and $[UO_2Cl_4]^{2-}$ calculated with time-dependent density functional theory. *J. Chem. Phys.*, 126(19):194311, 2007. doi: http://dx.doi.org/10.1063/1.2735297. URL http://scitation.aip.org/content/aip/journal/jcp/126/19/10.1063/1.2735297.

[34] Pawel Tecmer, Andre Severo Pereira Gomes, Ulf Ekstrom, and Lucas Visscher. Electronic spectroscopy of UO_2^{2+}, NUO^+ and NUN: an evaluation of time-dependent density functional theory for actinides. *Phys. Chem. Chem. Phys.*, 13:6249–6259, 2011. doi: 10.1039/C0CP02534H. URL http://dx.doi.org/10.1039/C0CP02534H.

[35] Pawel Tecmer, Niranjan Govind, Karol Kowalski, Wibe A. de Jong, and Lucas Visscher. Reliable modeling of the electronic spectra of realistic uranium complexes. *J. Chem. Phys.*, 139(3):034301, 2013. doi: 10.1063/1.4812360. URL `http://scitation.aip.org/content/aip/journal/jcp/139/3/10.1063/1.4812360`.

[36] Patrick Norman, David M. Bishop, Hans Jørgen Aagaard Jensen, and Jens Oddershede. Near-resonant absorption in the time-dependent self-consistent field and multiconfigurational self-consistent field approximations. *J. Chem. Phys.*, 115:10323, 2001.

[37] Patrick Norman, David M. Bishop, Hans Jørgen Aagaard Jensen, and Jens Oddershede. Nonlinear response theory with relaxation: the first hyperpolarizability. *J. Chem. Phys.*, 123:194103, 2005. doi: 10.1063/1.2107627.

[38] J. Autschbach, L. Jensen, G. C. Schatz, Y. C. E. Tse, and M. Krykunov. Time-Dependent Density Functional Calculations of Optical Rotatory Dispersion Including Resonance Wavelengths as a Potentially Usedful tool for Determining Absolute Configurations of Chiral Molecules. *J. Phys. Chem. A"*, 110:2461, 2006. doi: 10.1021/jp054847z.

[39] A Devarajan, A Gaenko, and J Autschbach. Two-component relativistic density functional method for computing nonsingular complex linear response of molecules based on the zeroth order regular approximation. *J. Chem. Phys.*, 130:194102, 2009. doi: 10.1063/1.3123765.

[40] Kasper Kristensen, Joanna Kauczor, Thomas Kjærgaard, and Poul Jørgensen. Quasienergy formulation of damped response theory. *J. Chem. Phys.*, 131(4):044112, 2009. doi: 10.1063/1.3173828. URL `http://scitation.aip.org/content/aip/journal/jcp/131/4/10.1063/1.3173828`.

[41] Sonia Coriani, Ove Christiansen, Thomas Fransson, and Patrick Norman. Coupled-cluster response theory for near-edge x-ray-absorption fine structure of atoms and molecules. *Phys. Rev. A*, 85:022507, Feb 2012. doi: 10.1103/PhysRevA.85.022507. URL `http://link.aps.org/doi/10.1103/PhysRevA.85.022507`.

[42] Hans Ågren, Vincenzo Carravetta, Olav Vahtras, and Lars G.M. Pettersson. Direct, atomic orbital, static exchange calculations of photoabsorption spectra of large molecules and clusters. *Chem. Phys. Lett.*, 222(1-2):75 – 81, 1994. ISSN 0009-2614. doi: http://dx.doi.org/10.1016/0009-2614(94)00318-1. URL `http://www.sciencedirect.com/science/article/pii/0009261494003181`.

[43] Vincenzo Carravetta and Hans Ågren. Computational x-ray spectroscopy. In Vincenzo Barone, editor, *Computational Strategies for Spectroscopy*, pages 137–205. John Wiley & Sons, Inc., 2011. ISBN 9781118008720. doi: 10.1002/9781118008720.ch3. URL `http://dx.doi.org/10.1002/9781118008720.ch3`.

[44] Hans Ågren, Vincenzo Carravetta, Lars G. M. Pettersson, and Olav Vahtras. Static exchange and cluster modeling of core electron shakeup spectra of surface adsorbates: Co/cu(100). *Phys. Rev. B*, 53:16074–16085, Jun 1996. doi: 10.1103/PhysRevB.53.16074. URL `http://link.aps.org/doi/10.1103/PhysRevB.53.16074`.

[45] T. Saue. Relativistic Hamiltonians for Chemistry: A Primer. *ChemPhysChem*, 12:3077, 2011. doi: 10.1002/cphc.201100682.

[46] Michael Dolg and Xiaoyan Cao. Accurate Relativistic Small-Core Pseudopotentials for Actinides. Energy Adjustment for Uranium and First Applications to Uranium Hydride. *J. Phys. Chem. A*, 113(45):12573–12581, 2009. doi: 10.1021/jp9044594. URL `http://pubs.acs.org/doi/abs/10.1021/jp9044594`. Pseudopotentials are available online at http://www.tc.uni-koeln.de/PP/clickpse.en.html.

[47] R A Evarestov, A I Panin, A V Bandura, and M V Losev. Electronic structure of crystalline uranium nitrides UN, U_2N_3 and UN_2 : LCAO calculations with the basis set optimization. *J. Phys. Conf. Ser.*, 117(1):012015, 2008. URL http://stacks.iop.org/1742-6596/117/i=1/a=012015.

[48] Laura Gagliardi and Björn O. Roos. Uranium triatomic compounds *XUY* (X,Y=C,N,O): a combined multiconfigurational second-order perturbation and density functional study. *Chem. Phys. Lett.*, 331(2-4):229 – 234, 2000. ISSN 0009-2614. doi: 10.1016/S0009-2614(00)01218-5. URL http://www.sciencedirect.com/science/article/pii/S0009261400012185.

[49] W. Küchle, M. Dolg, H. Stoll, and H. Preuss. Energy-adjusted pseudopotentials for the actinides. Parameter sets and test calculations for thorium and thorium monoxide. *J. Chem. Phys.*, 100(10):7535–7542, 1994. doi: 10.1063/1.466847. URL http://scitation.aip.org/content/aip/journal/jcp/100/10/10.1063/1.466847. Pseudopotentials are available online at http://www.tc.uni-koeln.de/PP/clickpse.en.html.

[50] M. Iliaš, H. J. Aa. Jensen, V. Kellö, B. O. Roos, and M. Urban. Theoretical study of PbO and the PbO anion. *Chem. Phys. Lett.*, 408:210, 2005. doi: http://dx.doi.org/10.1016/j.cplett.2005.04.027. URL http://www.sciencedirect.com/science/article/pii/S0009261405005440.

[51] W. Kutzelnigg and W. Liu. Quasirelativistic theory equivalent to fully relativistic theory. *J. Chem. Phys.*, 123:241102, 2005. doi: 10.1063/1.2137315. URL http://scitation.aip.org/content/aip/journal/jcp/123/24/10.1063/1.2137315.

[52] M. Iliaš and T. Saue. An infinite-order two-component relativistic Hamiltonian by a simple one-step transformation. *J. Chem. Phys.*, 126:064102, 2007. doi: 10.1063/1.2436882. URL http://dx.doi.org/10.1063/1.2436882.

[53] Rob Klooster, Ria Broer, and Michael Filatov. Calculation of X-ray photoelectron spectra with the use of the normalized elimination of the small component method. *Chem. Phys.*, 395:122 – 127, 2012. ISSN 0301-0104. doi: 10.1016/j.chemphys.2011.05.009. URL http://www.sciencedirect.com/science/article/pii/S0301010411001637. Recent Advances and Applications of Relativistic Quantum Chemistry.

[54] Michael J. Van Stipdonk, Maria del Carmen Michelini, Alexandra Plaviak, Dean Martin, and John K. Gibson. Formation of Bare UO_2^{2+} and NUO^+ by Fragmentation of Gas-Phase Uranyl-Acetonitrile Complexes. *J. Phys. Chem. A*, 118(36):7838–7846, 2014. doi: 10.1021/jp5066067.

[55] Tu Zhe-Yan, Yang Dong-Dong, Wang Fan, and Li Xiang-Yuan. A CCSD(T) Study on Structures and Harmonic Frequencies of the Isoelectronic Uranium Triatomic Species OUO^{2+}, NUN and NUO^+. *Acta Phys. Chim. Sin.*, 28(07):1707, 2012. doi: 10.3866/PKU.WHXB201205111. URL http://www.whxb.pku.edu.cn/EN/abstract/article_28085.shtml. (in Chinese).

[56] Rodney D. Hunt, Jason T. Yustein, and Lester Andrews. Matrix infrared spectra of NUN formed by the insertion of uranium atoms into molecular nitrogen. *J. Chem. Phys.*, 98(8):6070–6074, 1993. doi: 10.1063/1.464845. URL http://scitation.aip.org/content/aip/journal/jcp/98/8/10.1063/1.464845.

[57] T. Koopmans. Über die Zuordnung von Wellenfunktionen und Eigenwerten zu den Einzelnen Elektronen Eines Atoms. *Physica*, 1(1-6):104 – 113, 1934. ISSN 0031-8914. doi: 10.1016/S0031-8914(34)90011-2. URL http://www.sciencedirect.com/science/article/pii/S0031891434900112.

[58] R. S. Mulliken. Quelques Aspects de la théorie des orbitales moléculaires. *J. Chim. Phys.*, 46: 497, 1949. for an English translation, see https://openlibrary.org/books/OL7214165M/Report_on_molecular_orbital_theory.

[59] P. S. Bagus. Self-Consistent-Field Wave Functions for Hole States of Some Ne-Like and Ar-Like Ions. *Phys. Rev.*, 139:A619–A634, Aug 1965. doi: 10.1103/PhysRev.139.A619. URL http://link.aps.org/doi/10.1103/PhysRev.139.A619.

[60] K. Siegbahn, C. Nordling, G. Johansson, J. Hedman, P. F. Hedén, K. Hamrin, U. Gelius, T. Bergmark, L. O. Werme, and Y. Baer. *ESCA applied to free molecules*. North-Holland, Amsterdam, 1969. URL https://books.google.fr/books?id=suPvAAAAMAAJ.

[61] K. Siegbahn. Electron spectroscopy - an outlook. *J. Electron. Spectrosc. Relat. Phenom.*, 5 (1):3 – 97, 1974. doi: 10.1016/0368-2048(74)85005-X. URL http://www.sciencedirect.com/science/article/pii/036820487485005X.

[62] J. Thyssen. *Development and Applications of Methods for Correlated Relativistic Calculations of Molecular Properties*. PhD thesis, University of Southern Denmark, 2001. see http://www.diracprogram.org/doku.php?id=dissertations.

[63] Paul S. Bagus and Henry F. Schaefer. Direct Near-Hartree-Fock Calculations on the 1s Hole States of NO^+. *J. Chem. Phys.*, 55(3):1474–1475, 1971. doi: 10.1063/1.1676248. URL http://scitation.aip.org/content/aip/journal/jcp/55/3/10.1063/1.1676248.

[64] J. Almlöf, P. Bagus, B. Liu, D. MacLean, U. Wahlgren, and M. Yoshimine. MOLECULE-ALCHEMY program package, IBM Research Laboratory, 1972. an on-line manual is found at http://k-sek01.t-komazawa.ac.jp/msekiya/alchemy/.

[65] Andrew T. B. Gilbert, Nicholas A. Besley, and Peter M. W. Gill. Self-Consistent Field Calculations of Excited States Using the Maximum Overlap Method (MOM). *J. Phys. Chem. A*, 112(50):13164–13171, 2008. doi: 10.1021/jp801738f.

[66] . DIRAC, a relativistic ab initio electronic structure program, Release DIRAC14 (2014), written by T. Saue, L. Visscher, H. J. Aa. Jensen, and R. Bast. with contributions from V. Bakken, K. G. Dyall, S. Dubillard, U. Ekström, E. Eliav, T. Enevoldsen, E. Faßhauer, T. Fleig, O. Fossgaard, A. S. P. Gomes, T. Helgaker, J. K. Lærdahl, Y. S. Lee, J. Henriksson, M. Iliaš, Ch. R. Jacob, S. Knecht, S. Komorovský, O. Kullie, C. V. Larsen, H. S. Nataraj, P. Norman, G. Olejniczak, J. Olsen, Y. C. Park, J. K. Pedersen, M. Pernpointner, R. di Remigio, K. Ruud, P. Sałek, B. Schimmelpfennig, J. Sikkema, A. J. Thorvaldsen, J. Thyssen, J. van Stralen, S. Villaume, O. Visser, T. Winther, and S. Yamamoto (see http://www.diracprogram.org).

[67] Lucas Visscher, Timothy J. Lee, and Kenneth G. Dyall. Formulation and implementation of a relativistic unrestricted coupled-cluster method including noniterative connected triples. *J. Chem. Phys.*, 105(19):8769–8776, 1996. doi: 10.1063/1.472655. URL http://scitation.aip.org/content/aip/journal/jcp/105/19/10.1063/1.472655.

[68] Walter J. Lauderdale, John F. Stanton, Jürgen Gauss, John D. Watts, and Rodney J. Bartlett. Many-body perturbation theory with a restricted open-shell Hartree–Fock reference. *Chem. Phys. Lett.*, 187(1):21 – 28, 1991. ISSN 0009-2614. doi: 10.1016/0009-2614(91)90478-R. URL http://www.sciencedirect.com/science/article/pii/000926149190478R.

[69] J. Olsen and P. Jørgensen. Linear and nonlinear response functions for an exact state and for an MCSCF state. *J. Chem. Phys.*, 82:3235, 1985. doi: 10.1063/1.448223.

[70] J. Olsen and P. Jørgensen. Time-dependent response theory with applications to self-consistent field and multiconfigurational self-consistent field wave functions. In D. R. Yarkoni, editor, *Modern Electronic Structure Theory*, Advanced Series in Physical Chemistry. World Scientific, 1995.

[71] R. Bast, H. J. Aa. Jensen, and T. Saue. Relativistic adiabatic time-dependent density functional theory using hybrid functionals and noncollinear spin magnetization. *Int. J Quant. Chem.*, 109:2091, 2009. doi: 10.1002/qua.22065. URL `http://dx.doi.org/10.1002/qua.22065`.

[72] Stephan Bernadotte, Andrew J. Atkins, and Christoph R. Jacob. Origin-independent calculation of quadrupole intensities in X-ray spectroscopy. *J. Chem. Phys.*, 137(20):204106, 2012. doi: 10.1063/1.4766359. URL `http://link.aip.org/link/?JCP/137/204106/1`.

[73] Nanna Holmgaard List, Joanna Kauczor, Trond Saue, Hans Jørgen Aagaard Jensen, and Patrick Norman. Beyond the electric-dipole approximation: A formulation and implementation of molecular response theory for the description of absorption of electromagnetic field radiation. *J. Chem. Phys.*, 142(24):244111, 2015. doi: 10.1063/1.4922697. URL `http://scitation.aip.org/content/aip/journal/jcp/142/24/10.1063/1.4922697`.

[74] B. Levy. Multi-configurational Self-Consistent Wavefunctions of Formaldehyde. *Chem. Phys. Lett.*, 4:17, 1969. doi: 10.1016/0009-2614(69)85022-0.

[75] P. Joergensen and J. Linderberg. Time-dependent hartree-fock calculations in the pariser-parr-pople model. applications to aniline, azulene and pyridine. *Int. J Quant. Chem.*, 4:587, 1970. doi: 0.1002/qua.560040606.

[76] E. Dalgaard and P. Joergensen. Optimization of orbitals for multiconfigurational reference states. *J. Chem. Phys.*, 69:3833, 1978. doi: 10.1063/1.437049.

[77] T. Saue and T. Helgaker. Four-component relativistic Kohn–Sham theory. *J. Comput. Chem.*, 23:814, 2002. doi: 10.1002/jcc.10066.

[78] O. Christiansen, P. Jørgensen, and C. Hättig. Response Functions from Fourier Component Variational Perturbation Theory Applied to a Time-Averaged Quasienergy. *Int. J. Quant. Chem.*, 68:1, 1998. ISSN 1097-461X. doi: 10.1002/(SICI)1097-461X(1998)68:1<1::AID-QUA1>3.0.CO;2-Z. URL `http://dx.doi.org/10.1002/(SICI)1097-461X(1998)68:1<1::AID-QUA1>3.0.CO;2-Z`.

[79] T. Saue. Post Dirac-Hartree-Fock Methods - Properties. In P. Schwerdtfeger, editor, *Relativistic Electronic Structure Theory. Part 1. Fundamentals*, page 332. Elsevier, Amsterdam, 2002.

[80] Sebastien Villaume, Trond Saue, and Patrick Norman. Linear complex polarization propagator in a four-component Kohn-Sham framework. *J. Chem. Phys.*, 133(6):064105, 2010. doi: 10.1063/1.3461163. URL `http://scitation.aip.org/content/aip/journal/jcp/133/6/10.1063/1.3461163`.

[81] M Stener, G Fronzoni, and M de Simone. Time dependent density functional theory of core electrons excitations. *Chem. Phys. Lett.*, 373(1-2):115 – 123, 2003. ISSN 0009-2614. doi: http://dx.doi.org/10.1016/S0009-2614(03)00543-8. URL `http://www.sciencedirect.com/science/article/pii/S0009261403005438`.

[82] U. Ekström. *Time-dependent molecular properties in the optical and x-ray regions.* PhD thesis, Linköping universitet, 2007. see http://www.diracprogram.org/doku.php?id=dissertations.

[83] P. G. Burke and Kenneth Smith. The Low-Energy Scattering of Electrons and Positrons by Hydrogen Atoms. *Rev. Mod. Phys.*, 34:458–502, Jul 1962. doi: 10.1103/RevModPhys.34.458. URL http://link.aps.org/doi/10.1103/RevModPhys.34.458.

[84] NF Mott and HSW Massey. *The Theory of Atomic Collisions*. Clarendon Press, Oxford, 1965. p. 523.

[85] H. S. W. Massey and C. B. O. Mohr. The Collision of Slow Electrons with Atoms. I. General Theory and Elastic Collisions. *Proc. R. Soc. A*, 136(829):289–311, 1932. ISSN 0950-1207. doi: 10.1098/rspa.1932.0082.

[86] Philip M. Morse and W. P. Allis. The Effect of Exchange on the Scattering of Slow Electrons from Atoms. *Phys. Rev.*, 44:269–276, Aug 1933. doi: 10.1103/PhysRev.44.269. URL http://link.aps.org/doi/10.1103/PhysRev.44.269.

[87] William J. Hunt and William A. Goddard III. Excited States of H_2O using improved virtual orbitals. *Chem. Phys. Lett.*, 3(6):414 – 418, 1969. ISSN 0009-2614. doi: http://dx.doi.org/10.1016/0009-2614(69)80154-5. URL http://www.sciencedirect.com/science/article/pii/0009261469801545.

[88] T.N. Rescigno and P.W. Langhoff. K-shell photoionization in molecular nitrogen. *Chem. Phys. Lett.*, 51(1):65 – 70, 1977. ISSN 0009-2614. doi: http://dx.doi.org/10.1016/0009-2614(77)85356-6. URL http://www.sciencedirect.com/science/article/pii/0009261477853566.

[89] P. W. Langhoff. Applications of the Stieltjes-Tchebycheff procedure for atomic and molecular photoionization calculations in Hilbert space. *Int. J Quant. Chem.*, 12(S11):301–310, 1977. ISSN 1097-461X. doi: 10.1002/qua.560120836. URL http://dx.doi.org/10.1002/qua.560120836.

[90] J. A. Sheehy, T. J. Gil, C. L. Winstead, R. E. Farren, and P. W. Langhoff. Correlation of molecular valence- and K-shell photoionization resonances with bond lengths. *J. Chem. Phys.*, 91(3):1796–1812, 1989. doi: 10.1063/1.457085. URL http://scitation.aip.org/content/aip/journal/jcp/91/3/10.1063/1.457085.

[91] Per-Olov Löwdin. Quantum Theory of Many-Particle Systems. I. Physical Interpretations by Means of Density Matrices, Natural Spin-Orbitals, and Convergence Problems in the Method of Configurational Interaction. *Phys. Rev.*, 97:1474–1489, Mar 1955. doi: 10.1103/PhysRev.97.1474. URL http://link.aps.org/doi/10.1103/PhysRev.97.1474.

[92] Ulf Ekström, Patrick Norman, and Vincenzo Carravetta. Relativistic four-component static-exchange approximation for core-excitation processes in molecules. *Phys. Rev. A*, 73:022501, Feb 2006. doi: 10.1103/PhysRevA.73.022501. URL http://link.aps.org/doi/10.1103/PhysRevA.73.022501.

[93] S. Dubillard, J.-B. Rota, T. Saue, and K. Faegri. Bonding analysis using localized relativistic orbitals: Water, the ultrarelativistic case and the heavy homologues H_2X, (X = Te, Po, eka-Po). *J. Chem. Phys.*, 124(15):154307, 2006. doi: 10.1063/1.2187001. URL http://link.aip.org/link/?JCP/124/154307/1.

[94] Gerald Knizia. Intrinsic Atomic Orbitals: An Unbiased Bridge between Quantum Theory and Chemical Concepts. *J. Chem. Theory Comp.*, 9(11):4834–4843, 2013. doi: 10.1021/ct400687b. URL http://pubs.acs.org/doi/abs/10.1021/ct400687b.

[95] H.-J. Werner, P. J. Knowles, R. Lindh, F. R. Manby, M. Schütz, P. Celani, T. Korona, A. Mitrushenkov, G. Rauhut, T. B. Adler, R. D. Amos, A. Bernhardsson, A. Berning, D. L. Cooper, M. J. O. Deegan, A. J. Dobbyn, F. Eckert, E. Goll, C. Hampel, G. Hetzer, T. Hrenar, G. Knizia, C. Köppl, Y. Liu, A. W. Lloyd, R. A. Mata, A. J. May, S. J. McNicholas,

W. Meyer, M. E. Mura, A. Nicklass, P. Palmieri, K. Pflüger, R. Pitzer, M. Reiher, U. Schumann, H. Stoll, A. J. Stone, R. Tarroni, T. Thorsteinsson, M. Wang, and A. Wolf. MOLPRO, version 2009.1, a package of ab initio programs. see http://www.molpro.net.

[96] Thom H. Dunning. Gaussian basis sets for use in correlated molecular calculations. I. The atoms boron through neon and hydrogen. *J. Chem. Phys.*, 90(2):1007–1023, 1989. doi: http://dx.doi.org/10.1063/1.456153. URL http://scitation.aip.org/content/aip/journal/jcp/90/2/10.1063/1.456153.

[97] R A Kendall, T H Dunning, and Robert J Harrison. Electron-affinities of the 1st-row atoms revisited - systematic basis-sets and wave-functions. *J. Chem. Phys.*, 96:6796, 1992. doi: http://dx.doi.org/10.1063/1.462569.

[98] . DIRAC, a relativistic ab initio electronic structure program, Release DIRAC13 (2013), written by L. Visscher, H. J. Aa. Jensen, R. Bast, and T. Saue, with contributions from V. Bakken, K. G. Dyall, S. Dubillard, U. Ekström, E. Eliav, T. Enevoldsen, E. Faßhauer, T. Fleig, O. Fossgaard, A. S. P. Gomes, T. Helgaker, J. K. Lærdahl, Y. S. Lee, J. Henriksson, M. Iliaš, Ch. R. Jacob, S. Knecht, S. Komorovský, O. Kullie, C. V. Larsen, H. S. Nataraj, P. Norman, G. Olejniczak, J. Olsen, Y. C. Park, J. K. Pedersen, M. Pernpointner, K. Ruud, P. Sałek, B. Schimmelpfennig, J. Sikkema, A. J. Thorvaldsen, J. Thyssen, J. van Stralen, S. Villaume, O. Visser, T. Winther, and S. Yamamoto (see http://www.diracprogram.org).

[99] Lucas Visscher. Approximate molecular relativistic Dirac-Coulomb calculations using a simple Coulombic correction. *Theor. Chem. Acc.*, 98(2-3):68–70, 1997. ISSN 1432-881X. doi: 10.1007/s002140050280. URL 10.1007/s002140050280.

[100] Kenneth G. Dyall. Relativistic double-zeta, triple-zeta, and quadruple-zeta basis sets for the actinides Ac-Lr. *Theor. Chem. Acc.*, 117(4):491–500, 2007. ISSN 1432-881X. doi: 10.1007/s00214-006-0175-4. URL http://dx.doi.org/10.1007/s00214-006-0175-4.

[101] L. Visscher and K.G. Dyall. Dirac-Fock atomic electronic structure calculations using different nuclear charge distributions. *At. Data Nucl. Data Tables*, 67(2):207 – 224, 1997. ISSN 0092-640X. doi: http://dx.doi.org/10.1006/adnd.1997.0751. URL http://www.sciencedirect.com/science/article/pii/S0092640X97907518.

[102] A. D. Becke. Density-functional exchange-energy approximation with correct asymptotic behavior. *Phys. Rev. A*, 38:3098–3100, Sep 1988. doi: 10.1103/PhysRevA.38.3098. URL http://link.aps.org/doi/10.1103/PhysRevA.38.3098.

[103] Chengteh Lee, Weitao Yang, and Robert G. Parr. Development of the Colle-Salvetti correlation-energy formula into a functional of the electron density. *Phys. Rev. B*, 37:785–789, Jan 1988. doi: 10.1103/PhysRevB.37.785. URL http://link.aps.org/doi/10.1103/PhysRevB.37.785.

[104] Burkhard Miehlich, Andreas Savin, Hermann Stoll, and Heinzwerner Preuss. Results obtained with the correlation energy density functionals of becke and Lee, Yang and Parr. *Chem. Phys. Lett.*, 157(3):200 – 206, 1989. ISSN 0009-2614. doi: http://dx.doi.org/10.1016/0009-2614(89)87234-3. URL http://www.sciencedirect.com/science/article/pii/0009261489872343.

[105] P. J. Stephens, F. J. Devlin, C. F. Chabalowski, and M. J. Frisch. Ab Initio Calculation of Vibrational Absorption and Circular Dichroism Spectra Using Density Functional Force Fields. *J. Phys. Chem.*, 98(45):11623–11627, 1994. doi: 10.1021/j100096a001. URL http://dx.doi.org/10.1021/j100096a001.

[106] Axel D. Becke. Density-functional thermochemistry. III. The role of exact exchange. *J. Chem. Phys.*, 98(7):5648–5652, 1993. doi: http://dx.doi.org/10.1063/1.464913. URL http://scitation.aip.org/content/aip/journal/jcp/98/7/10.1063/1.464913.

[107] John P. Perdew, Kieron Burke, and Matthias Ernzerhof. Generalized Gradient Approximation Made Simple. *Phys. Rev. Lett.*, 77:3865–3868, Oct 1996. doi: 10.1103/PhysRevLett.77.3865. URL http://link.aps.org/doi/10.1103/PhysRevLett.77.3865.

[108] Carlo Adamo and Vincenzo Barone. Toward reliable density functional methods without adjustable parameters: The PBE0 model. *J. Chem. Phys.*, 110(13):6158–6170, 1999. doi: 10.1063/1.478522. URL http://link.aip.org/link/?JCP/110/6158/1.

[109] Takeshi Yanai, David P Tew, and Nicholas C Handy. A new hybrid exchange-correlation functional using the Coulomb-attenuating method (CAM-B3LYP). *Chem. Phys. Lett.*, 393 (1-3):51 – 57, 2004. ISSN 0009-2614. doi: http://dx.doi.org/10.1016/j.cplett.2004.06.011. URL http://www.sciencedirect.com/science/article/pii/S0009261404008620.

[110] Xiaoyan Cao, Michael Dolg, and Hermann Stoll. Valence basis sets for relativistic energy-consistent small-core actinide pseudopotentials. *J. Chem. Phys.*, 118(2):487–496, 2003. doi: 10.1063/1.1521431. URL http://scitation.aip.org/content/aip/journal/jcp/118/2/10.1063/1.1521431. Pseudopotentials are available online at http://www.tc.uni-koeln.de/PP/clickpse.en.html.

[111] Xiaoyan Cao and Michael Dolg. Segmented contraction scheme for small-core lanthanide pseudopotential basis sets. *J. Mol. Struct. (Theochem)*, 581(1-3):139 – 147, 2002. ISSN 0166-1280. doi: 10.1016/S0166-1280(01)00751-5. URL http://www.sciencedirect.com/science/article/pii/S0166128001007515.

[112] Pekka Pyykko and Leif Laaksonen. Relativistically parameterized extended Hueckel calculations. 8. Double-.zeta. parameters for the actinoids thorium, protactinium, uranium, neptunium, plutonium, and americium and an application on uranyl. *J. Phys. Chem.*, 88 (21):4892–4895, 1984. doi: 10.1021/j150665a017.

[113] R.G. Denning. Electronic structure and bonding in actinyl ions. In *Complexes, Clusters and Crystal Chemistry*, volume 79 of *Structure and Bonding*, pages 215–276. Springer Berlin Heidelberg, 1992. ISBN 978-3-540-55095-2. doi: 10.1007/BFb0036502. URL http://dx.doi.org/10.1007/BFb0036502.

[114] F. Hund. Zur Frage der chemischen Bindung. II. *Zeitschrift fÃŒr Physik*, 73(9-10):565–577, 1932. ISSN 1434-6001. doi: 10.1007/BF01342005. URL http://dx.doi.org/10.1007/BF01342005.

[115] R. S. Mulliken. Spectroscopy, molecular orbitals and chemical bonding. *Science*, 157:13, 1967.

[116] J. Pipek and P. G. Mezey. A fast intrinsic localization procedure applicable for *ab initio* and semiempirical linear combination of atomic orbital wave functions. *J. Chem. Phys.*, 90: 4916, 1989.

[117] Evelyn Sokolowski, Carl Nordling, and Kai Siegbahn. Chemical Shift Effect in Inner Electronic Levels of Cu Due to Oxidation. *Phys. Rev.*, 110:776–776, May 1958. doi: 10.1103/PhysRev.110.776. URL http://link.aps.org/doi/10.1103/PhysRev.110.776.

[118] Stig Hagström, Carl Nordling, and Kai Siegbahn. Electron spectroscopic determination of the chemical valence state. *Z. Phys.*, 178(5):439–444, 1964. ISSN 0044-3328. doi: 10.1007/BF01379473. URL http://dx.doi.org/10.1007/BF01379473.

[119] P. Indelicato and E. Lindroth. Relativistic effects, correlation, and QED corrections on K α transitions in medium to very heavy atoms. *Phys. Rev. A*, 46:2426–2436, Sep 1992. doi: 10.1103/PhysRevA.46.2426. URL http://link.aps.org/doi/10.1103/PhysRevA.46.2426.

[120] T. Mooney, E. Lindroth, P. Indelicato, E. G. Kessler, and R. D. Deslattes. Precision measurements of K and L transitions in xenon: Experiment and theory for the K , L , and M levels. *Phys. Rev. A*, 45:1531–1543, Feb 1992. doi: 10.1103/PhysRevA.45.1531. URL http://link.aps.org/doi/10.1103/PhysRevA.45.1531.

[121] Indelicato, P., Boucard, S., and Lindroth, E. Relativistic and many-body effects in K, L, and M shell ionization energy for elements with $10 \leq Z \leq 100$ and the determination of the 1s Lamb shift for heavy elements . *Eur. Phys. J. D*, 3(1):29–41, 1998. doi: 10.1007/s100530050146. URL http://dx.doi.org/10.1007/s100530050146.

[122] Marcel Nooijen and Rodney J. Bartlett. Description of core-excitation spectra by the open-shell electron-attachment equation-of-motion coupled cluster method. *J. Chem. Phys.*, 102 (17):6735–6756, 1995. doi: 10.1063/1.469147. URL http://scitation.aip.org/content/aip/journal/jcp/102/17/10.1063/1.469147.

[123] J. A. Bearden and A. F. Burr. Reevaluation of X-Ray Atomic Energy Levels. *Rev. Mod. Phys.*, 39:125–142, Jan 1967. doi: 10.1103/RevModPhys.39.125. URL http://link.aps.org/doi/10.1103/RevModPhys.39.125.

[124] Robert G. Denning. Electronic Structure and Bonding in Actinyl Ions and their Analogs. *J. Phys. Chem.*, 111(20):4125–4143, 2007. doi: 10.1021/jp071061n.

[125] I Cacelli, V Carravetta, A Rizzo, and R Moccia. The calculation of photoionisation cross sections of simple polyatomic molecules by L^2 methods. *Phys. Rep.*, 205(6):283 – 351, 1991. ISSN 0370-1573. doi: 10.1016/0370-1573(91)90041-J. URL http://www.sciencedirect.com/science/article/pii/037015739190041J.

[126] Ulf Ekström and Patrick Norman. X-ray absorption spectra from the resonant-convergent first-order polarization propagator approach. *Phys. Rev. A*, 74:042722, Oct 2006. doi: 10.1103/PhysRevA.74.042722. URL http://link.aps.org/doi/10.1103/PhysRevA.74.042722.

[127] Guangde Tu, Vincenzo Carravetta, Olav Vahtras, and Hans Ågren. Core ionization potentials from self-interaction corrected Kohn-Sham orbital energies. *J. Chem. Phys.*, 127(17):174110, 2007. doi: 10.1063/1.2777141. URL http://scitation.aip.org/content/aip/journal/jcp/127/17/10.1063/1.2777141.

[128] Andreas Dreuw, Jennifer L. Weisman, and Martin Head-Gordon. Long-range charge-transfer excited states in time-dependent density functional theory require non-local exchange. *J. Chem. Phys.*, 119(6):2943–2946, 2003. doi: 10.1063/1.1590951. URL http://scitation.aip.org/content/aip/journal/jcp/119/6/10.1063/1.1590951.

[129] D. P. Chong, O. V. Gritsenko, and E. J. Baerends. Interpretation of the Kohn–Sham orbital energies as approximate vertical ionization potentials. *J. Chem. Phys.*, 116(5):1760–1772, 2002. doi: 10.1063/1.1430255. URL http://scitation.aip.org/content/aip/journal/jcp/116/5/10.1063/1.1430255.

[130] O. V. Gritsenko, B. BraÃ¯da, and E. J. Baerends. Physical interpretation and evaluation of the Kohn–Sham and Dyson components of the ε–I relations between the Kohn–Sham orbital energies and the ionization potentials. *J. Chem. Phys.*, 119(4):1937–1950, 2003. doi: 10.1063/1.1582839. URL http://scitation.aip.org/content/aip/journal/jcp/119/4/10.1063/1.1582839.

[131] Oleg Gritsenko and Evert Jan Baerends. The analog of Koopmans' theorem for virtual Kohn–Sham orbital energies. *Can. J. Chem.*, 87(10):1383–1391, 2009. doi: 10.1139/V09-088. URL http://www.nrcresearchpress.com/doi/abs/10.1139/V09-088.

[132] M. O. Krause and J. H. Oliver. Natural widths of atomic K and L levels, Kα X-ray lines and several KLL Auger lines. *J. Phys. Chem. Ref. Data*, 8(2):329–338, 1979. doi: 10.1063/1.555595. URL http://scitation.aip.org/content/aip/journal/jpcrd/8/2/10.1063/1.555595.

[133] K. Hämäläinen, D. P. Siddons, J. B. Hastings, and L. E. Berman. Elimination of the inner-shell lifetime broadening in x-ray-absorption spectroscopy. *Phys. Rev. Lett.*, 67:2850–2853, Nov 1991. doi: 10.1103/PhysRevLett.67.2850. URL http://link.aps.org/doi/10.1103/PhysRevLett.67.2850.

[134] Yu Zhang, Jason D. Biggs, Daniel Healion, Niranjan Govind, and Shaul Mukamel. Core and valence excitations in resonant X-ray spectroscopy using restricted excitation window time-dependent density functional theory. *J. Chem. Phys.*, 137(19):194306, 2012. doi: http://dx.doi.org/10.1063/1.4766356. URL http://scitation.aip.org/content/aip/journal/jcp/137/19/10.1063/1.4766356.

[135] Michael Roemelt, Dimitrios Maganas, Serena DeBeer, and Frank Neese. A combined DFT and restricted open-shell configuration interaction method including spin-orbit coupling: Application to transition metal L-edge X-ray absorption spectroscopy. *J. Chem. Phys.*, 138 (20):204101, 2013. doi: http://dx.doi.org/10.1063/1.4804607. URL http://scitation.aip.org/content/aip/journal/jcp/138/20/10.1063/1.4804607.